Transition Metal Atoms Pathways on Rutile TiO_2 (110) Surface: Distribution of Ti^{3+} States and Evidence of Enhanced Peripheral Charge Accumulation

Yongqing Cai[1], Zhaoqiang Bai[1], Sandhya Chintalapati[1], Qingfeng Zeng[2], and Yuan Ping Feng[1]*
[1]*Department of Physics, National University of Singapore, 2 Science Drive 3, Singapore 117542, Singapore*
[2]*School of Materials Science and Engineering, Northwestern Polytechnical University, Xi'an 710072, China*
(Dated: October 31, 2012)

Charge transfer between metal nanoparticles and the supported TiO_2 surface is primarily important for catalytic applications as it greatly affects the catalytic activity and the thermal stability of the deposited nanoparticles on the surface. Herein, a systematic spin-polarized density functional calculation is performed to evaluate the adsorption, diffusion, and charge state of several transition metal monomers on both stoichiometric and reduced rutile TiO_2 (110) surface. The role of oxygen vacancy (O_v) with its accompanying excess electrons in influencing the activation of the monomers is examined. For pristine reduced surface, our hybrid functional calculation shows that only a small portion (around 5%) of the excess electrons occupy the topmost surface, which are mainly delocalized at the second nearest and third nearest fivefold coordinated Ti (Ti_{5c}) atoms. The small amounts of excess electrons populating at the Ti_{5c} atoms can be transferred to strongly electronegative adsorbates like Au and Pt thus enabling a moderate adsorption, whereas no stable adsorption at the Ti_{5c} site is found for other less electronegative TM adatoms(Ag, Cu, Fe, Co, Ni and Pd) on the reduced surface and for all the adatoms on stoichiometric surface. This finding clarify the origin of the experimental observation of the adsorption of O_2 and CO molecules at Ti_{5c} sites in connection with charge transfer. In addition, the spatial redistribution of the excess electrons at Ti_{5c} sites around the O_v upon the adsorption of the monomers is thoroughly examined. Our finding of an accumulation of excess electrons at the Ti_{5c} sites around the monomers explains the critical role of the perimeter interface of the deposited nanoparticles in promoting the adsorption and activation of reactants observed in experiments.

I. INTRODUCTION

Transition metal (TM) nanoparticles dispersed on oxide substrates exhibit extraordinary high catalytic activity for various low-temperature oxidation processes,[1,2] which has inspired extensive studies on the synthesis of these hybrid materials with controlled structures and the mechanisms of the promoted catalytic activity. Among several oxide substrates studied, TM clusters supported on TiO_2 surface[3,4] attract enhanced attention due to their strong oxidizing power and nontoxicity, and applications in heterogeneous catalysis, photocatalysis, solar cells, and gas sensors.[5–7] The adsorbed TM clusters provide versatile functionalities such as activating the adsorbed species, generating peripheral interface as active sites for CO and NO oxidation,[8,9] and enhancing the kinetics of charge transfer and suppressing electron/hole recombination for photocatalysis applications.[10,11]

Catalytic performance of supported TM particles is found to be remarkably sensitive to their sizes.[12,13] Haruta found a strong catalytic activity of Au nanoclusters dispersed on the rutile TiO_2 particles only appears for Au clusters with the size below 5 nm.[14] For Pd deposited titania surface, the changes in electronic structures give rise to strong size variations in CO oxidation activity.[15] Unfortunately, the deposited TM clusters usually tend to rearrange themselves and grow even at moderate temperature for several TM clusters such as Ag,[16] Cu,[17] Au,[18,19] Pd,[20] and Pt,[21] and thus reducing their activity and reusability under ambient condition. Hence, a detailed understanding of the factors influencing the thermally-driven coarsening of deposited clusters and diffusion kinetics of TM monomers is vital to the control of the size of clusters during growth,[22–25] prehibiting cluster coarsening and finding effective ways of redispersion[9,26–28] of the TM particles for real applications.

Another central issue of concern in engineering metal/oxide interfaces is to understand and control the interfacial interaction between the oxide and deposited particles. Upon depositing TM nanoparticles on the surface, the electronic properties of the TiO_2 surface are altered where Schottky barrier and band bending appear near the interface region.[29,30] This significantly affects the trapping and subsequent transfer of photoexcited electrons on the TiO_2 surface for photocatalysis of water-splitting.[10,31] Photoelectron measurements have revealed that new electronic states may be formed in the surface-band-gap of TiO_2 which can be either characteristics of TM states or reduced Ti 3+ or 2+ states due to redox reaction at the interface between TM and TiO_2.[32,33] On the other hand, the interfacial interaction between the two phases can render the deposited TM clusters negatively or positively charged,[34] which is a key factor influencing the catalytic ability of the catalysis. A negatively charged state of Au clusters deposited on oxide F centers was reported to be the underlying reason for a highly catalytic ability for low temperature CO oxidation.[35] However, reports of charge state of deposited TM clusters

*Electronic address: phyfyp@nus.edu.sg

are often controversial due to uncertainties related to the presence of defect on the surface and the size variation of the deposited cluster.

Among the various surface structural defects on the TiO_2 surface, oxygen vacancy (O_v) is the most abundant one and significantly affects the surface chemistry and electronic properties of the surface.[23,36] The presence of one neutral O_v leaves behind two excess electrons which tend to transfer to the unoccupied 3*d* orbitals of Ti atoms and thus making the surface reduced and simultaneously inducing Ti^{3+} defective states. Although the energetic positions of the Ti^{3+} states are unambiguously determined to locate in the band gap about 0.9 eV below the conduction band minimum according to photoelectron spectrum of the reduced TiO_2 surfaces,[23,36,37] the exact spatial location of the excess electrons associated with O_v is still under debate.[38–41] One would expect that these excess electrons are located at neighboring cation atoms near the O_v,[39,40,42–44] however, recent experiments show that the electron is more likely to be localized primarily outside O_v.[45,46,48] As reactants tend to be trapped and activated in the electron accumulated region of the surface, the understanding of the spatial distribution of the excess charge is highly important.[23,49–51] Upon depositing TM nanoparticles on the surface that nucleation preferentially appear on defect sites, charge transfer may occur at the interface and a great interest lies in the investigation of the redistribution of the defective states which has been still unknown.

For understanding the above issues in the TM/TiO_2 system, density-functional-theory (DFT) calculations play an important role in exploring the TM interaction with the surface and further the catalytic mechanisms.[22,23] The credibility of normal DFT based on single-particle approximations has been extensively shown for obtaining binding energy and structural properties.[52–54] However, the deficiency in the exchange-correlation functionals makes the calculated band gap severely underestimated, which does not allow a proper description of the energetic alignment of TM localized states with the TiO_2 bulk extending states.[23] The lack of self-interaction corrections even fail to reproduce electronic features of the highly delocalized defective states related to the O_v in TiO_2.[55] Moreover, the different models and methods adopted in previous studies do not allow a quantitative comparison of the stability and mobility of TM monomers on titania surface. In this study, we systematically investigate the interaction of TM monomers with the TiO_2 (110) surface. The studied TM species include 3*d* (Fe, Co, Ni, Cu), 4*d* (Pd, Ag), and 5*d* (Pt, Au) which span a broad range of atoms with different degree of interactions with the surface according to Diebold.[22] Special attention is focused on the interfacial interaction and the redistribution of charges at the interface. Clearly, the modification of the diffusion barrier and charging state of TM monomer due to the presence of O_v varies with the TM identity. We quantify the redistribution of excess charge around the defective center due to TM adsorption.

II. COMPUTATIONAL DETAILS AND SURFACE MODEL

To simulate the interaction of TM adatoms with the TiO_2 (110) surface, a periodic slab of three layers of O-Ti_2O_2-O units (9 atomic layers) has been used. Each slab is separated by a vacuum of 12 Å normal to the surface. Atoms in the two lowest atomic layers (the most far away from the adatom) were fixed at their bulk positions, and others were allowed to relax. The lattice constant of the TiO_2 (110) surface unit cell are c and $\sqrt{2}a$ along [001] and $[1\bar{1}0]$ directions respectively, $a = 4.57$ Å and $c = 2.94$ Å being the two lattice constants of the rutile TiO_2. A (4×2) surface supercell (four unit cells in the [001] direction and two in the $[1\bar{1}0]$ direction) was used. Thus one TM adatom per supercell gives 1/8 ML coverage.

All our calculations were performed using the plane-wave code Vienna ab initio simulation package (VASP)[56] within the framework of DFT in combination of both the generalized gradient approximation (GGA) and hybrid functionals. Spin-polarized calculations using the projector augmented wave method with the Perdew-Burke-Ernzerhof functional (PAW-PBE)[57] were performed. A cutoff energy of 400 eV and Γ point sampling in k-space were adopted. Structures were relaxed until the Hellmann-Feynman forces become less than 0.01 eV/Å. For examining the binding and diffusion of TM on the TiO_2 surface, the GGA calculation was performed which has been extensively employed for investigating adatom and molecule interaction with the TiO_2 surfaces.

To calculate the full migration energy profiles of TM on the surface, the potential energy surface (PES) was calculated through sampling certain surface area. For the stoichiometric surface, a rectangular region defined by dimensions of $c/2$ along [001] direction and $a/\sqrt{2}$ along $[1\bar{1}0]$ direction, as plotted in Fig. 1, was divided into a 8×15 uniform grid. The TM adatom at each grid point was fixed in the in-plane directions and allowed to relax only in the direction normal to the surface. The PES on the whole surface was then generated through considering the symmetry of the surface. To investigate the diffusion of TM monomer on a partially reduced surface with missing oxygen atoms, a partially reduced surface was created by removing every other oxygen atom in each row of bridging oxygen along [001] direction. The vacancy concentration produced in this way is 0.5 ML which corresponds to a strongly reduced surface. As there are numerous geometrical configurations of a reduced surface defined by the distribution and the concentration of the bridging O_v's, the present reduced surface model allows us to take advantage of the symmetry and minimize the number of sampling images while ensuring a high resolution for the PES plot. A rectangular region defined by dimensions of c along [001] direction and $a/\sqrt{2}$ along $[1\bar{1}0]$ direction was then divided into a 10×15 uniform

grid.

To obtain an accurate picture of electronic interaction for TM's adsorbed on the TiO_2 surface and simultaneously explore the effect of O_v on the TMs adsorption, we make use of hybrid functionals (HSE06),[58] in which part of the semilocal exchange-correlation functional is substituted by the Hartree-Fock exchange. Since the hybrid functional approach is computationally more expensive, only the most stable binding configuration and other metastable structures determined from the PES obtained by the GGA calculation, were calculated with the hybrid functional approximation. In addition, to improve the inaccuracy in structural relaxation due to lack of electronic self-interaction for describing systems with localized d electrons, the relaxed atomic structures by GGA calculation were further optimized by using a GGA + U approach before hybrid functional calculation. The effective on-site Coulomb parameters (U) are $U = 5.8$ eV for Ti $3d$ and $U = 5.0$ eV for TM d electrons.[59] Based on the hybrid functional results, the electron density differences, $\Delta\rho$, were calculated via

$$\Delta\rho \;=\; \rho_{\mathrm{TM/surface}} - (\rho_{\mathrm{TM}}^{\mathrm{frozen}} + \rho_{\mathrm{surface}}^{\mathrm{frozen}}) \qquad (1)$$

where $\rho_{\mathrm{TM/surface}}$ is the electron density for the TM adatom-surface system in its stablest configuration, $\rho_{\mathrm{TM}}^{\mathrm{frozen}}$ and $\rho_{\mathrm{surface}}^{\mathrm{frozen}}$ are the electron densities of the TM adatom and the surface kept frozen in the positions of the adatom-surface system, respectively. The isosurface value of the electron density differences for all the TM cases is kept to be 0.03 to enable a direct comparison.

III. RESULTS

A. Pristine s-TiO_2 and r-TiO_2 (110) surface

Before presenting the results of TM adsorption and diffusion on the stoichiometric (s-TiO_2) and reduced (r-TiO_2) surfaces, we first analyze the structural and electronic properties of the pristine surfaces. The surface plane of the s-TiO_2 (110) surface is composed of alternating atomic rows of twofold coordinated bridging O^{2-} (O_{2c}) and fivefold coordinated Ti^{4+} (Ti_{5c}) ions in the [001] direction (Fig. 1). There exist two types of Ti atoms and two types of O atoms: fivefold coordinated Ti sites (Ti_{5c}), sixfold coordinated Ti sites (Ti_{6c}), twofold coordinated bridging O atoms (O_{2c}) and threefold coordinated in-plane O atoms (O_{3c}). Several high-symmetry sites for TM adsorption can be identified as follow: top of bridging O atom, center between two O_{2c} atoms (B_o), centers of triangles (T_1 and T_2) formed by O_{2c} and O_{3c}, hollow (H) over two Ti_{5c} atoms and two O_{2c} atoms at the basal plane. The r-TiO_2 surface is created by removing O_{2c} atoms which possess relatively small defect formation energy compared to O_{3c} atoms. The original Ti_{6c} atoms bound to the removed O_{2c} become fivefold coordinated, denoted as Ti_{6c}(d).

The electronic density of state (DOS) for the pristine surface is compared with that of the rutile TiO_2 bulk. As shown in Fig. 2, the band gap value for the bulk is calculated to be 3.0 eV which is in good agreement with experimental results.[22] The valence band is predominantly O $2p$ derived and the conduction band is Ti $3d$ derived. Using nomenclature from molecular-orbital theory and in accordance with the literature,[60] the valence band can be further divided into "bonding" (the bottom of the valence band between -7 and -4 eV) and "nonbonding" (the top of the valence band between -4 and -1 eV) parts concerning the strength of hybridization of O-$2p$ and Ti-$3d$ states. For the s-TiO_2 surface, the summed local density of state (LDOS) of the topmost O-Ti_2O_2-O layer is plotted in Fig. 2b. As in the bulk case, the valence band is mainly O-$2p$ derived and the conduction band is mainly Ti-$3d$ derived, however, there is an increased bonding between the surface O and Ti atoms, as evidenced by a broadening "bonding" part in the LDOS, to compensate the decrease of coordination number in surface atoms.

For the defective r-TiO_2 surface, to minimize the O_v-O_v interaction, we take a single O_v on the (4×2) surface. It is well known that reduction of TiO_2 surface through creation of O_v on the surface leads to formation of defective states with Ti $3d$ character at about 1.0 eV below the bottom of the conduction band. Although these defect states in the band gap are clearly visible in spectroscopies, standard GGA-DFT calculations fail to produce the exact energetic location of the band-gap defective states due to deficiencies in the functionals.[55] Based on the hybrid functional corrections, as plotted in Fig. 3a and b, our results show a spin-triplet paramagnetic state composed of two spin-unpaired states locating at 0.8 and 1.4 eV below the conduction band minimum, which agrees fairly well with experimental observations.[22,23] Surprisingly, the calculated occupations of two states in the LDOS projected on the topmost layer only amount to 0.08 electron, which suggests that only around 5% of the two excess electrons locates in the topmost surface layer. Combining DFT+U and the Car-Parrinello molecular dynamics, Kowalski et al.[38] have also found that the surface layer is only occupied by the excess electrons about 20% of time and the subsurface is populated about 70% of time. This strong difference in lifetime occupying these two layers shows a strong preference for populating sites in the subsurface layer. A more recent study[61] demonstrates that the spatial distribution of the excess electrons on the TiO_2 (110) surface is independent of the way excess electrons are produced.

In addition to predict the exact energetic location of the reduced states,[62] many theoretical and experimental studies have been devoted to understanding the degree of localization and the exact spatial distribution of these states on the topmost surface layer which have been a subject of debate.[42,63–67] Some early experiments and theoretical calculations show that the excess electrons populate the $3d$ unoccupied orbitals of the Ti ions (Ti_{6c}(d)) adjacent to the O_v's.[39,40,42] However, these

findings are inconsistent with the observations in a STM study of CO adsorption showing that the next-nearest-neighbor Ti_{5c} sites (Ti_{5c1}(d)) of O_v are the most stable binding sites for CO and the excess charge is localized primarily outside the O_v.[45] Similarly, recent experiments showed that O_2 can adsorb and dissociate at Ti_{5c} sites on reduced surfaces without direct interaction of O_2 with O_v.[46,47] To clearly understand the spatial distribution of the band-gap states, we plot the LDOS of the three types of Ti_{5c} atoms (Ti_{6c}(d), Ti_{5c1}(d), Ti_{5c2}(d) as labeled in Fig. 1) around the O_v in Fig. 3c. Note that the LDOS for each type is a summation of the LDOS of symmetrically equivalent atoms around the O_v. The population of each in-gap state is calculated by integrating the peaks. The result shows that there is no defective state within the band gap for Ti_{6c}(d). This indicates that the excess charge is not localized in the nearest Ti_{6c}(d) ions of the O_v defect, rather most (about 80%) of the excess electron in the topmost layer is centered on Ti_{5c1}(d) and Ti_{5c2}(d) ions around the O_v. Our finding is in good agreement with recent atomic-scale resolution occupied-state STM and STS measurements which show that the neighboring Ti_{6c}(d) ions can not hold electrons.[48] The four bright lobes around the O_v site in the measurement indicates a distribution of electrons on the Ti sites in the basal plane. Based on resonant photoelectron diffraction measurements,[63] Kruger et al. also found that most of the charge is distributed on the Ti_{5c}(d) ions around the O_v and only a small fraction is located on Ti ions directly underneath the O_v.

Since O_v's are ubiquitous on the oxide surface and greatly influence the catalysis activity or the solar adsorption efficiency of nanoparticle/TiO_2 hybrid system, the interplay between the defects and deposited nanoparticles is critical for applications.[23,55,68] According to our above analysis, the excess electrons can not be trapped at the defect center or the nearest Ti atoms, and the top TiO_2 surface trilayer attracts only about 5% of the excess electrons from the O_v. The questions naturally arise in nanoparticle/TiO_2 systems: How does the defective states evolve when a TM adatom is adsorbed on the O_v site? Does it still locate on the Ti_{5c1}(d) and Ti_{5c2}(d) atoms or evolve back to the nearest Ti_{6c}(d) atom or even transfer to the adsorbate? It would be very interesting to see how the adatoms influence the distribution of the excess electrons around the O_v. In the following sections, we touch upon these issues and focus on the electronic interaction between the TM adatoms and TiO_2 surface, which is enabled by the advanced hybrid functional calculation.

B. Au, Ag, and Cu adatom on s-TiO_2 and r-TiO_2 surface

Cu: Figure 4a shows the PES for a single Cu adatom on the s/r-TiO_2 (4×2) surface. The PES is plotted with reference to the lowest TM adsorption energy on the surface. On the stoichiometric surface, as shown in Fig. 4a, the Cu energy profile varies significantly on the surface. The barrier to migrate along the [001] direction is 0.64 eV, whereas the diffusion barrier along the [1$\bar{1}$0] direction is 1.45 eV. Such a strong difference in the activation energy along the two directions suggests different hopping rates for Cu diffusion and a preferable formation of Cu clusters along the [001] direction. The most stable adsorption site is found to be the B_o site (Table. I) with the adsorption energy of 2.75 eV which is in good agreement with previous calculated value of 2.85 eV.[52] In the most stable configuration, the Cu adatom binds to two bridging O_{2c} atoms with Cu-O_{2c} distance of 1.86 Å. This value is more approximate to the Cu-O bond length for bulk Cu_2O (1.85 Å) than that for bulk CuO (1.96 Å).[69] In addition, the twofold coordinated Cu adatom between the two O_{2c} atoms is similar to the O-Cu-O zigzag frameworks in bulk Cu_2O.[70] Therefore, we conclude that, for the initial growth of Cu on TiO_2, the interface structure and the oxidation state (shown below) of Cu on TiO_2 resembles the case of Cu_2O. Our result is in good agreement with previous experimental studies of the local structure of Cu/TiO_2 interface.[69,71–73] Surface x-ray diffraction study shows that Cu adsorption induces large vertical and lateral displacements of O atoms indicating a substantial degree of Cu-O bonding.[69] XAFS measurement shows that Cu atoms bind to two bridging oxygen atoms with a bond length of 1.84 Å[71] and no direct Cu-Ti bonding is observed.[72]

On the reduced surface, the diffusion barriers for Cu to move out of the O_v are calculated to be 1.00 and 1.45 eV along [001] and [1$\bar{1}$0] direction, respectively. The most favorable site for Cu adsorption is the O_v site (Table. II). The calculated binding energy of 1.92 eV is lower by around 0.8 eV compared to that of the adsorption on the s-TiO_2 surface. Contrary to the common notion that the O_v on the surface can anchor the adatom more strongly, the presence of O_v defect on the TiO_2 surface decreases the Cu/TiO_2 interaction. This finding is consistent with the experimental observation that defects on the TiO_2 surface have negligible effect on the growth of Cu.[17]

The different adsorption behavior of Cu on s-TiO_2 and r-TiO_2 originates from a different electronic interaction between Cu/TiO_2 interaction for the two cases. Figure 4b shows the charge density difference between the adatom and surface. For the Cu/s-TiO_2, the singly occupied outer 4s electron tends to transfer to the TiO_2 surface. Bader charge analysis shows that about 0.8 electron is transferred from Cu to s-TiO_2 surface making Cu positively charged, whereas about 0.3 electron is transferred from the electron-rich r-TiO_2 surface to the Cu adatom making Cu slightly negatively charged. Figure 4c shows the LDOS of Cu and atoms on the topmost O-Ti_2O_2-O layer. The interaction of Cu with the s-TiO_2 surface makes the initially singly occupied 4s state of Cu empty, and the hybridization with O_{2c} atoms makes Cu 3d orbitals split into two peaks: one about 0.3 eV above the valence band maximum, and the other one ranging

from 1.5 to 6 eV below Fermi level (E_f) locates at the valence band top. This is consistent with UPS spectrum that records a new sharp peak at around 2.5 eV below E_f and a continuous suppression of the substrate emission from the O $2p$ valence band from 3 to 8 eV below E_f upon deposition of Cu on TiO_2(110) surface.[74] Nakajima[33] also observed two peaks at about 2.8 eV and 0.8 eV below E_f, where the former is assigned to the Cu oxidation state (Cu $3d^{10}$) consistent with our result, however, the latter is ascribed to the reduced Ti $3d$ state. According to our calculation, we cannot observe any reduced state and thus the peak at 0.8 eV should originate from the Cu $3d$ in-gap state. For Cu/r-TiO_2 interaction, in addition to several defective in-gap states of the surface, there occurs a sharp state in the band gap from the TiO_2 surface being resonance with Cu $4s$ state. According to our results shown in Sect. 1, there is no excess charge occupying the Ti_{6c}(d) site. Upon Cu adsorption at the O_v site, however, some excess electrons are firstly transferred to Ti_{6c}(d) $3d$ orbitals and finally form bonds with the $4s$ electron of Cu atom as shown in the charge transfer plot in Fig. 1b and LDOS in Fig. 4e. The excess electron screens the Cu atom and weakens the interaction between Cu and the surface which explains the smaller binding energy compared to the stoichiometric surface.

Ag: Ag adatom exhibits similar adsorption and diffusion behaviors on the TiO_2 surfaces with Cu. The most stable adsorption site on the stoichiometric surface is the B_o site with both the adsorption energy (1.72 eV) and the diffusion barriers (0.26 eV for [001] direction and 0.91 eV for [1$\bar{1}$0] direction, see Fig. 5a) being much smaller than those of Cu. The weaker interaction is accompanied by a slightly smaller amount of charge transfer (0.78 e) from Ag $5s$ state to the surface (Fig. 5b). As in the Cu case, the binding energy (1.37 eV) for the r-TiO_2 case is smaller than that on the s-TiO_2 surface due to the excess-charge screening of the Ag atom. For s-TiO_2 surface, unlike the Cu case, LDOS calculation shows that Ag $4d$ orbitals span from 1.7 to 6 eV below E_f and locate completely within the valence band. There is no in-gap state as observed in the Cu/s-TiO_2 system. On the reduced surface, the diffusion barrier of Ag is much higher compared with the stoichiometric surface. The charge transfer from the surface makes the adatom negatively charged (-0.24 e). LDOS plot shows that the Ag $5s$ state is partially populated with the excess electron and locates in the band gap being nearer to the conduction band bottom than Cu $4s$ state (Fig. 3e). The overlap of the Ag $5s$ state and Ti $3d$ defective state has been observed in experiment.[16]

Our results are in good agreement with other studies[16,52,75] and can reasonably explain some experimental observations for Ag nanoparticles decorated on TiO_2 surface.[16,75–77] STM images[75] shows that the Ag monomer binds on the bridging oxygen rows twice as often as on the Ti rows which can be explained by the larger binding energy (Fig. 5a) through bonding with O_{2c} atoms. Diffusion of Ag clusters and the effects of defects on the TiO_2 surface have also been investigated.[76] The experiment found that Ag atoms travel faster in the direction parallel to the bridging-oxygen rows, which is due to a much smaller diffusion barrier along the [001] direction according to our result (Fig. 5a). A weak interaction was observed between Ag and O_v[76] which is consistent with our result showing a smaller Ag/r-TiO_2 binding energy. More recently, the structural evolution, epitaxy, and sublimation temperature of silver nanoclusters on TiO_2 surface have been thoroughly studied.[77] A remarkable difference in the behavior of Ag on oxidized and reduced surface was found. The Ag sublimation temperature in the case of Ag nanoclusters on reduced TiO_2 is smaller than oxidized TiO_2 surface[77] again supporting our result of a weaker interaction for Ag bound on O_v site.

Au: Au clusters have attracted great interest since the discovery of surprisingly high catalytic reactivity when they are highly dispersed on metal oxides (TiO_2, Fe_2O_3, MgO, etc.).[78–80] Defects like O_v on the surface play a predominant role in charging and activating the Au clusters to give rise to the high catalytic ability.[79,80] The energy maps for Au diffusing on the stoichiometric and reduced TiO_2 surface are shown in Fig. 6a. On the s-TiO_2 surface, the most favorable site is the atop site of O_{2c}. In this configuration, the Au-O_{2c} bond distance is 1.98 Å which matches well with XANES measured Au-O bond length of 1.95 Å.[81] The binding energy is calculated to be 1.02 eV, which is smaller than those of Ag and Cu on s-TiO_2 surface. The activation energies for Au hopping through the two successive minimums are 0.16 eV along [001] direction and 0.57 eV along [1$\bar{1}$0] direction, respectively, showing a preferential growth along [001].[64,82] On the reduced r-TiO_2 surface, the binding energy of Au adsorption on the O_v site increases to 2.55 eV, which is in contrast to Cu and Ag where adsorption on O_v site has a smaller binding energy than on stoichiometric surface. In addition, the energy barrier for diffusion increases significantly, up to 2.13 eV along [001] direction and 1.34 eV along [1$\bar{1}$0] direction. Our results showing a stronger interaction for adsorption on the r-TiO_2 surface are in agreement with other DFT studies[18,53,54,83,84,86,87] and experimental observation of Au adsorption on TiO_2 (110) surface.[88] In addition to the O_v site, we also identify a local minimum (Fig. 6a) on the Ti_{5c2}(d) site with a adsorption energy of 1.28 eV, about 1.27 eV lower compared with adsorption at the O_v site. The presence of this stable adsorption site suggests a possibility of forming a bond between Au and Ti_{5c2}(d) which is absence for the above Ag and Cu cases(Fig. 4a and Fig. 5a). According to our above analysis, the excess electrons are mainly accumulated on the Ti_{5c1}(d) and Ti_{5c2}(d) sites. A high electronegativity of the Au atoms (6.06 eV) allows a charge transfer from the Ti_{5c} sites of n-typed defective r-TiO_2 surface which has a smaller work function (4.4 eV) than that of s-TiO_2 surface (5.8 eV). This explains why no such local minimum is present on s-TiO_2 surface. Similarly, as shown below, for Pt adatom with a

large electronegativity (6.06 eV), a stable adsorption at the Ti_{5c2}(d) site also occurs on the r-TiO_2 surface.

Figure 6b shows the charge transfer between Au and TiO_2 surfaces. The isosurface plot for Au/s-TiO_2 shows an apparent polarized character of the Au-O_{2c} bond. The electrons transferred from the Au singly occupied 6s state to the surface amounts to 0.63 e, slightly smaller than the values of Cu (0.80 e) and Ag (0.78 e). In contrast, the binding of Au on O_v site leads to a reverse electron transfer from the surface to the Au atom with Au negatively charged (-0.51 e). On the experimental side, the charge transfer between Au and s-TiO_2 or r-TiO_2 surface has been observed by detecting the changes of the work function,[90,91] XPS shift,[92] surface band bending[93] of the Au adsorbed TiO_2 surface or monitoring the vibration frequency[94] of the CO molecule adsorbed on the supported Au clusters. The reverse trend in the charge transfer for s-TiO_2 and r-TiO_2 surfaces is also reflected in the LDOS plots (Fig. 6c). For s-TiO_2 surface, there are two peaks in the LDOS plot of Au at -2.2 eV and -3.5 eV located within the valence band of TiO_2. Our orbital analysis shows that the former is a Au 6s-5d hybridized state which is contrast to Ag and Cu adsorbed on s-TiO_2 where no s state locates beneath the E_f. For the r-TiO_2 surface, a significant effect is that the initially half-filled 6s state of Au becomes almost completely filled due to the charge transfer from the surface. The alignment of Au states with the valence band of the surfaces correlates well with those recorded XPS spectra for Au/TiO_2 system.[90,95–97]

In summary, for Ag, Cu, and Au atoms, all of them have a $nd^{10}(n+1)s^1$ configuration with a half-filled $(n+1)s$ state. After adsorption on the TiO_2 surface, the singly occupied state can either be nearly empty by donating the single electron to the stoichiometric surface having a larger work function, or be nearly completely filled through accepting excess electron from the reduced surface having a smaller work function. This dynamical modulation of the valence states of these species gives rise to the drastically different adsorption and diffusion behaviors on s-TiO_2 and r-TiO_2 surfaces, and may be the reason of the high catalytic performance of the decorated surfaces for a wealth of reactions such as the water-gas shift reaction[12] and CO oxidation.[51,98] For adsorption on r-TiO_2 surface, the interaction between adatom and the surface causes a shift of orbital levels of all of the adatoms as compared to adsorption on s-TiO_2 surface. For all the three cases, the adhesion of adatoms on O_v site induces the electrons accumulated between the adatom and the two titanium atoms next to the vacancy. These accumulated electrons disturb the Ti-O structure around the cluster that provides new adsorption site for molecules, and therefore the perimeter interface of the adatoms or clusters plays an important role in activating the molecules during chemical reactions.

C. Fe, Co, and Ni adatom on s-TiO_2 and r-TiO_2 surface

In this part, we study the interaction of Fe, Co and Ni adatoms with the TiO_2 (110) surface. Due to a similar electronic configuration, the three VIII-group elements have similar characteristics for adsorption and diffusion on the surface. Since all the three atoms have strong reactivity toward oxygen, they show much stronger interactions than the above IB atoms (Cu, Ag, and Au). Despite their important applications, theoretical calculations on the adsorption and diffusion properties on the TiO_2 surface have less been performed.

Fe: On the s-TiO_2 surface, the PES for Fe diffusion is shown in Fig. 7a and the most stable adsorption is found to be the T_1 site being in line with the experimental observation by Diebold et. al.[32] The Fe atom is coordinated with 3 oxygen atoms with two types of Fe-O bonds (Table. I). The adsorption energy on this site is calculated to be 4.54 eV which is the largest adsorption energy among all the studied adatoms. For adsorption on r-TiO_2 surface, the PES is highly corrugated and the energy minimum locates near the O_v site. In comparison with the s-TiO_2 surface, the binding energy at the O_v site is 2.57 eV, about 2 eV smaller, and the diffusion barriers increase along the [001] direction and decrease along the [1$\bar{1}$0] direction. Thus the presence of O_v enhances the mobility of Fe diffusing across the terrace. It is important to note that the real diffusion barriers for Fe monomer hopping between successive stable sites may be smaller than the value shown in the PES plot as the Fe adatom may not directly move along the lines. Nevertheless, the activation energies along the two directions are still meaningful to compare the mobility of Fe atoms on different surfaces. Our findings of a weaker interaction on the reduced surface can well explain some phenomena previously observed.[99,100] Pan et.al.[99] have observed that Fe films wet better on a partially reduced surface than on the stoichiometric surface. They ascribed this to a stronger bonding at the interface due to O_v defect on the surface, however, according to our calculation, the Fe/r-TiO_2 interface has a weaker interaction and the improved wetting behavior should be a kinetics effect related to a higher Fe diffusion rate due to a lower diffusion barrier. The high diffusion barrier on the s-TiO_2 surface is also supported by the experiment findings by Mostéfa-Sba et. al.[100] who found that for a high initial roughness of the substrate, a two-dimensional growth mode is observed up to three monolayers, but clusters grow on the TiO_2 surface if the initial roughness is low.

Figure 6b plots the isosurface of charge transfer between Fe and TiO_2 surfaces. Bader charge analysis shows a charge transfer of 1.48 electron from Fe to s-TiO_2 surface. Surprisingly, for Fe adsorption on r-TiO_2 surface, in contrast to most of the adatoms where electrons are transferred from r-TiO_2 surface to adatoms, Fe still donates its electrons to the r-TiO_2 surface although the amount of transferred charge is much smaller than at the

Fe/s-TiO_2 interface. The reason can be related to the electronegativity of Fe which is even smaller than that of r-TiO_2 (110) surface. Our finding is in good agreement with experimental observations. XPS results show that the oxidation of Fe atoms on the partially reduced surface still occurs,[99] and the amount of electrons exchanged between titanium and iron is lower when the substrate oxide surface is prereduced.[100]

With respect to the electronic structure of Fe/TiO_2 system, XPS studies show that there are emission peaks related to in-gap states which are believed to be the Ti^{3+} reduced states.[32,74,99,101] However, controversy still exists regarding the origin of these states. The reduced state can be produced either due to charge transfer from Fe to substrate Ti ions as observed for alkali atoms on TiO_2 surface, or physical removal of oxygen from the surface which occurs for strong reactive metal overlayers.[32] In order to clarify this uncertainty, we plot the LDOS of Fe in Fig. 7c-e. For Fe on s-TiO_2 surface, we can not observe any in-gap states near the bottom of conduction band. Thus we may exclude the possibility of charge-transfer induced Ti^{3+} reduced states and the emission peaks arise from the change of O_{2c} positions at the interface. However, considering the significant charge transfer from Fe to s-TiO_2 surface and a strong polaronic behavior of electrons on the surface, at finite temperature, both the above effects may coexist and contribute to the recorded Ti^{3+} reduced states.

Co: The ground state electronic configuration of Co atom is $3d^74s^2$. There are two types of cobalt oxide-CoO and Co_3O_4-with oxidation state of Co ranging form Co^{2+} to Co^{4+}. Upon adsorption of Co on the TiO_2 surface, the Co atom is prone to be oxidized by the oxygen atom on the surface and it is important to determine the oxidation state of Co and local structure at the interface. The adsorption and diffusion of Co on TiO_2 surface are quite similar to the above Fe case except a weaker interaction. For Co on s-TiO_2 surface, as shown in Fig. 8a, the diffusion barriers along [001] and [1$\bar{1}$0] directions are smaller than those of Fe diffusing on the surface. The most stable adsorption site is on the T_1 site. The Co atom is coordinated with two O_{2c} atoms and one O_{3c} atom and the Co-O distances are 1.83 and 1.98 A, respectively, which are similar to the Co-O bond length (1.928 Å) in $[Co^{2+}O_4]$ tetrahedron in Co_3O_4. Our predicted Co-O bond length is in good agreement with EXAFS measured Co-O distance (1.93 Å).[102] Similar to Fe case, when O_v is present on the surface, the binding energy of Co adsorption on the r-TiO_2 surface decreases, and the diffusion barrier increases along the [001] direction and decreases along the [1$\bar{1}$0] direction compared to those of adsorption on s-TiO_2 surface. Y. Shao[103] compared the stability of Co on fully oxidized and partially reduced TiO_2 surfaces and found that the Co layer is less stable on the partially reduced support than on fully oxidized titania which is in good agreement with our results.

The isosurface of charge transfer is plotted in Fig. 8b. In case of Co/s-TiO_2 system, Bader charge analysis shows that about 1.37 electrons are transferred from Co to s-TiO_2 surface. Therefore, both charge transfer analysis and the local structure of adsorbed Co indicate that the oxidized Co atom is likely to be in the Co^{2+} state and Co/s-TiO_2 interface adopts a tetrahedra structure as in Co_3O_4. LDOS (Fig. 8c) projected on Co atom shows that the cobalt 3d states are strongly hybridized with the whole valence band of oxygen 2p states. There is no in-gap state induced by Co. For Co/r-TiO_2 system, the net charge transfer from Co to r-TiO_2 surface is negligible and the Co atom remains nearly neutral. LDOS plot (Fig. 6d and e) shows that there are two different occupied states close to E_f: one is the Ti $3d^1$ state of Ti^{3+}, the second one is related to Co. In the experiment conducted by Y. Shao,[103] a new peak at about 1.45 eV below E_f for the reduced surface was observed when compared to the stoichiometric surface, which however was not well understood. Based on our calculation, this state should be Co-related gap states due to spin-split of Co 3d level.

Ni: Several studies have been dedicated to the energetics, structures, and magnetic properties of Ni clusters on TiO_2 surface.[104–106] It is found that Ni clusters tend to reside at the step edges, implying that the metal atoms are mobile enough on the surface to diffuse to the most favorable binding sites at the step edges.[106] The reactivity of nickel towards TiO_2 surface is still subject to debate. XPS study shows that only about 0.1 electron per Ni atom is transferred to the TiO_2 surface indicating a weak reduction of the surface.[107] However, the charge transfer is recently found to be highly dependent on the size of the Ni layer and the stoichiometry of the TiO_2 surface.[108]

The PES for Ni diffusion on s-TiO_2 and r-TiO_2 surface is shown in Fig. 9a. Compared to Fe and Co, the diffusion barriers along [001] and [1$\bar{1}$0] directions are evidently smaller. The most stable binding site is the B_o site with the adsorption energy of 3.71 eV, smaller than those of Fe and Co. The Ni atom is twofold coordinated and bound with two O_{2c} atoms with the Ni-O distance of 1.81 Å, in line with EXAFS measured value (1.84 Å),[110] suggesting the formation of NiO at the interface. The results are consistent with other experimental observations.[111,112]

Our charge transfer analysis (Fig. 9b) shows that about 0.85 electron from Ni is donated to the s-TiO_2 surface. This is supported by a reduced work function of the adsorbed surface detected through UPS.[113] However, the trend of charge transfer reverses for Ni anchored at O_v site on r-TiO_2 surface, and the electron flows from the surface to Ni adatom making it negatively charged ($Ni^{-0.52}$), which is contrast to the positively charged state for Fe and neutral state for Co at O_v site. The LDOS for Ni/s-TiO_2 and Ni/r-TiO_2 is plotted in Fig. 9c-e. For both cases, the result shows that there are Ni states in the band gap, which makes it difficult to justify the presence of the possible Ti^{3+} in-gap reduced state from experiment.[33,107,108,113] Our results clearly show that there is no Ti^{3+} state in the band gap for Ni/s-TiO_2 system. For Ni adsorbed on r-TiO_2 system, the Ni

$3d$ states are pushed away the E_f due to a filling of $4s$ state through accepting electrons from the surface.

Comparing with the IB elements (Cu, Ag, Au), the three VIII B elements (Fe, Co, and Ni) possess larger oxygen affinity. The behavior of binding energy of Fe, Co, and Ni on the s-TiO_2 surface follows: Fe > Co > Ni, whereas the trend reverses for adsorption on the reduced surface. In addition, the presence of O_v on the surface also affects the diffusion barriers: comparing with s-TiO_2 surface, the diffusion barrier along [001] on r-TiO_2 surface increases and the degree of increase follows the trend: Ni > Co > Fe, whereas the diffusion barrier along $[1\bar{1}0]$ decreases and the degree of decrease follows: Ni < Co < Fe. This clearly shows that O_v's have strong effect on changing the diffusion behavior on the surface. The underling mechanism is related to the difference of the electronegativity of the elements and will be discussed below.

D. Pd and Pt adatom on s-TiO_2 and r-TiO_2 surface

Pd: Noble metals like Pd and Pt are typical elements with strong metal substrate interaction (SMSI) effect when adsorbed on TiO_2 surface.[114,115] To gain an insight into the mobility of Pd monomer on the TiO_2 surface and evaluate the effect of O_v defect, we calculated the PES for Pd diffusing on s-TiO_2 and r-TiO_2 surfaces as shown in Fig. 10a. On the s-TiO_2 surface, the most favorite binding site is the B_o site with the Pd-O bonding length of 2.08 Å and the binding energy of 1.94 eV which is in good agreement with the results given by Kawazoe's group.[116] The barriers to migrate along the [001] and $[1\bar{1}0]$ directions are about 0.45 eV, which suggests a relatively weak interaction and a high diffusion rate at room temperature.[117–119] On the r-TiO_2 surface, the interaction between Pd and the surface is much stronger. The most stable site is the O_v site and the binding energy increases by 0.47 eV compared with adsorption on s-TiO_2 surface. The diffusion barriers are enhanced accordingly (Fig. 10a). Our result is consistent with other theorectical findings[68,120,121] and experimental reports showing that the O_v defects hinder diffusion and slow down particle growth.[122]

The Pd monomer is slightly positively charged ($Pd^{0.72+}$) when deposited on the s-TiO_2 surface through donating the electron to the surface. On reduced surface, electrons flow in the opposite direction when the adatom is bound to the O_v site. Since the electronic configuration of Pd adopts $4d^{10}$ and the $4d$ orbitals are fully occupied, the electron transferred from the r-TiO_2 surface tends to populate the $5s$ and $4p$ orbitals as in the Ag case, and the plot of isosurface of charge transfer for Pd/r-TiO_2 (shown in Fig. 10b) is similar to the IB atoms (Au, Cu, Ag) on the reduced TiO_2 surface. Therefore, a similar electronic structure property and chemical functionality of Pd and IB atoms on the r-TiO_2 surface is predicted. This explains why an equally high catalytic ability for CO oxidation is observed for Pd clusters as supported Au clusters.[15]

Photoelectron spectroscopy measurement of the initial growth of Pd on TiO_2 surface shows a shoulder in the valence band.[20] In Fig. 10c-e, we plot the LDOS for deposited Pd monomer. On the s-TiO_2 surface, there are Pd $4d$ related hybridized states located at the top of valence band. In line with previous experimental studies,[20,114,118] no reduction of the Ti^{+4} on the surface is found. On the r-TiO_2 surface, due to electron transferred from the surface, there occurs one $5s$-$4p$ hybridized state at -1 eV.

Pt: Pt has a large electronegativity and is expected to effectively enhance the photocatalytic activity of TiO_2. The catalytic activity of Pt cluster depends strongly on oxidation state of the cluster and the dimensions of the cluster.[34] A geometrical transition from a planar structure to a three dimensional structure was observed when the cluster size increases to 8 Pt atoms.[123] It evolves into SMSI state when the pre-adsorbed TiO_2 oxide surface is reduced.[115,124,125] Understandings of the adsorption site, diffusion kinetics, interfacial interaction, and O_v's effect are critical for controlling the cluster size and improving the catalytic performance.[123]

The calculation of PES (Fig. 11a) for Pt on the TiO_2 surface allows us to identify all the possible energetically favorable binding sites.[126] In contrast to other TM atoms which generally have only one stable binding site on the surface, for Pt on the s-TiO_2 surface, it is clear that there are two stable adsorption geometries, termed as B_o site and T_2 site, respectively, which are nearly energetically degenerate with a similar binding energy (2.66 eV at B_o site and 2.59 eV at displaced T_2 site). At the B_o site, Pt adatom is bonded to two bridging O_{2c} atoms with a distance of 1.93 A, whereas at T_2 site Pt is bonded to one O_{2c} atom (Pt-O bond length: 2.02 Å) and one Ti_{5c} atom (Pt-Ti bond length: 2.63 Å). While the adsorption at T_2 site was reported in previous DFT studies, the most energetically favorable B_o site was missing.[127,128] On the reduced surface, the most favorable adsorption is at the O_v site and the calculated binding energy is 4.64 eV, about 2 eV larger than adsorption on the s-TiO_2 surface being consistent with other findings.[21,130] As found in Au case, there is also a relatively weaker adsorption at the Ti_{5c2}(d) site due to accumulation of excess electrons at this site. The diffusion barrier on the reduced surface is nearly 3 times larger than that on the stoichiometric surface which suggests O_v has a significant effect on the stability and mobility of Pt adatoms.

The calculated adsorption configurations are in good agreement with the experiment conducted by Onishi's group to determine the Pt binding sites through detecting the perturbation of local work function due to Pt adatoms on the surface.[131] They identified three adsorption sites: a 4-fold hollow site, an O_v site, and a bridge site between two O_{2c} atoms. According to our calculation, the assumed 4-fold hollow site that describes Pt anchored between the O atom rows should be more likely

to be the T_2 site. They also found that Pt located at O_v are less mobile than other two cases, which is consistent with the significantly larger activation energy for adsorption at O_v site. However, the author claims an electron transfer from Pt to O_v site which is inconsistent with our study showing that the Pt is negatively charged at O_v site.

For Pt on both s-TiO_2 and r-TiO_2 surfaces, there are in-gap states about 1 eV above the valence band, which are predominantly Pt 5d orbitals slightly hybridized with 2p orbital of O_{2c} or 3d orbital of Ti_{5c}(d). On the s-TiO_2 surface, about 0.64 and 0.11 electron is donated to the surface upon Pt adsorption at B_o site and T_2 site, respectively. The different amounts of charge transfer induce a different degree of reduction of local work functions thus enabling the identification of the two Pt binding sites.[113,131] On the r-TiO_2 surface, the trend of charge transfer reverses. The intrinsic Ti^{3+} states on the reduced surface are significantly suppressed due to significant charge transfer from the surface to Pt adatom (Fig. 11b).[133–136] Bader charge analysis shows that Pt is negatively charged ($Pt^{0.96-}$) and forms strong Pt-Ti bonds with a mixture of ionic and covalent characteristics. This charge transfer greatly contributes to the formation of SMSI state through the diffusion of subsurface cation atoms. The direction and the amount of charge transfer are well reflected from the observed modulation of work function of the surface.[113,130,131] Upon reducing the Pt-decorated s-TiO_2 surface through annealing in the vacuum, some positive shifts of work function[113] and quenching of the Ti^{3+} defective state[137] of the pre-reduced surface occur, which can be explained by our result of the charge transfer from Ti cations to the Pt. Unlike Au, the charge transfer per Pt atom seems to be less dependent on the size of the cluster.[113]

IV. DISCUSSION

A. Charge State and Binding Energy of Deposited TM Monomer

The charge state of TM clusters plays a key role in determining the catalytic ability and thermal stability of the clusters deposited on the surface.[15,36] It is found that charging of the TM clusters helps to activate the adsorbed molecules through populating anti-bonding orbitals and decrease the reaction barrier.[35] The accumulated electrons on the TM clusters can facilitate the charge transfer to protons during water splitting.[10] Negative (positive) charge states of TM nanoparticles promote the metal oxidation (encapsulation) at the interface.[138] However, for most of the TM clusters, their exact charge states whether they are negatively charged, positively charged or keeping metallic are under intense debate.[22] Identifying the factors influencing the oxidation state of the deposited nanoparticles on oxide surfaces is not only industrially important but also of profound fundamental interest.

The direction of charge transfer can be predicted through comparing the electronegativity of the TM adsorbate with the work function of the surface.[139] This suggests that the degree of charge transfer is affected by both the TM species and the oxidation state of the surface. Electrons tend to flow from species with smaller electronegativity to species with larger electronegativity. This is indeed observed in our calculation. The amount of charge transfer between the metal adatoms and the TiO_2 surface is summarized in Fig. 12a. The alignment of the electronegativity of TM adatom with the work function of stoichiometric and reduced TiO_2 surface is plotted in Fig. 12b. On the stoichiometric surface, all the TM monomers donate some electrons to the surface as most of the TM species are less electronegative than the surface. Fe adatom with the smallest electronegativity shows the largest electron donation, whereas Pt and Au with a large electronegativity are only slightly positively charged. For the reduced surface, the removal of oxygen atoms causes the electrons originally bound to the oxygen to delocalize on the surface, which tend to transfer to TM adsorbates. The required charge-neutrality condition shifts the Fermi level toward the vacuum level and thus a smaller work function for the reduced surface. This implies the possibility of making adsorbed TM species negatively charged.

Due to the charge transfer at the TM/oxide interface, the chemical and electronic properties of both the surface and the deposited clusters are changed which enables the detection of the charge state of deposited TM clusters.[140] Several experimental approaches have been proposed and applied to determine the charge state of deposited TM particles. First, the electron transfer at the interface causes the initial state effect in XPS spectrum, and the shift of the TM related peaks has been widely used to probe the charging state of the TM clusters.[33,92] Second, in the presence of charge transfer, the work function of the surface is modified due to the electric dipole moment created at the surface[141] and has been used to quantitatively estimate the charge transfer for Ni,[107] Pt,[113,130,131] Au[90,91] nanoparticles on the surface. The variation of local work function on the deposited surface has been measured to pinpoint the exact binding sites of Pt adatoms,[131] and the findings are consistent with our PES result. In addition, the charge transfer induces band bending on the TiO_2 surface. Recording the rigid shifts of substrate core levels is an effective method to obtain the charge states of the clusters.[17,93] Finally, detecting a softening or hardening character of the vibrational frequencies of the adsorbed molecules on decorated surfaces can be used to deduce the charge state of the TM clusters.[94,142] The charge state of Au atoms was determined by measuring the CO frequency as rather different CO frequencies appear after adsorbing on oxidized, neutral or reduced gold particles.[12,143]

Our calculated charge states of the TM monomers are in line with the experimental observations. Surprisingly,

the dramatically different charge states of TM clusters on stoichiometric and reduced surface can be well reproduced by our calculations for TM monomers. However, it should be noted that, with increasing the size of the clusters, the amount of charge transfer on each atom tends to decrease accordingly.[17,108,141] This is because the energy penalty of repulsive interaction between TM ions outweighs the energy decrease arising from chemical hybridizations. The lower charge state of each TM atom in large clusters may explain why a lower catalytic performance often occurs when the size of the deposited cluster increases.

The binding energy for the adsorption of TM monomer on TiO_2 surface is closely related to the charge transfer at the interface. Contributions of interfacial interaction can be divided into two parts, a chemically covalent bonding part and an electrostatic interaction part, where the latter is directly related to the amount of charge on the interfacial atoms. Several studies have established the relationship between electronegativity of an adsorbate deposited on TiO_2 surface, which closely correlates the charge transfer with the adsorption energy.[30,144] In Fig. 13, we summarize the binding energy for all the TM monomers on both s-TiO_2 and r-TiO_2 surface. Combined with the plot of charge transfer in Fig. 12a, we can see that a larger amount of charge on the TM atom associated with a larger binding energy due to a stronger chemical reaction and electrostatic interaction. For Au, Ag and Cu all having a singly occupied outer s electron, the different ability of donating this electron to the stoichiometric surface gives rise to different binding energy. For Au and Pt, due to a pronounced charge transfer, the adsorption energy on the reduced surface is greatly enhanced. For Ag, Cu and the VIIIB TM atoms (Fe, Co, Ni), a weaker interaction is predicted for adsorption on reduced surface than on stoichiometric surface.

B. Stability and Effect of O_v

The stability of a TM adatom describing the ability of the adatom to displace away from the most favorable geometry is an important parameter for the growth and the thermal stability of the TM clusters. For real applications the size of the clusters should be controlled and cluster sintering after deposition should be suppressed during real catalytic processes.[27,28,49,78] There are two main coarsening mechanisms: Ostwald ripening, in which TM atoms detach from smaller clusters and diffuse on the surface until they join larger clusters, and diffusion coalescence, where larger clusters are formed by diffusing the entire smaller clusters.[25,146] The energy for the detachment of a single atom from the deposited clusters, the strength of cluster-oxide interfacial bonding, and the diffusion kinetics of involved species determine the specific type of the coarsening pathway for the chosen materials system.[146] As the diffusion rate of a dimer or a trimer is supposed to be very slow, diffusion of monomer on the TiO_2 surface dominates the growth-kinetics behavior of TM cluster and the trend of cluster sintering and coalescence. Under the same surface model, our calculation shows that the activation barrier of TM monomers for diffusion correlates well to their binding energy: VIIIB TM adatoms (Fe, Co, Ni) with unfilled $3d$ states generally has much larger bind energy and activation energy than adatoms in the IB group (Cu, Ag, and Au) and Pd monomer with a fully filled nd^{10} configuration.

It is expected that those factors influencing the binding energy should also play a role in modifying the activation energy for atomic diffusion. The presence of O_v which decreases the work function and provides the excess electrons on the surface has been shown to greatly change the charge transfer between the adsorbates and the surface.[36] For Au and Pt adatoms with a large electronegativity, such a upward shift of the Fermi level causes strongly different charge flow compared with perfect surface and allows additional anchoring site at the Ti_{5c} sites around O_v. The general belief is that O_v serves as trapping sites and the diffusion of TM monomer slows down due to a stronger interaction and a larger barrier. While this is indeed the case for the noble metals like Au, Pd, and Pt, for VIIIB elements: Fe, Co and Ni, the interfacial interaction becomes weaker at O_v site and the activation energy decreases accordingly. One possible reason for this weakening effect is that the excess electrons are transferred to the anti-bonding orbitals of the interfacial TM atoms thus decreasing the interfacial interaction. For Ag and Cu adatoms deposited on the reduced surface, the binding energy slightly decreases whereas the diffusion barrier slightly increases. The underlying mechanisms of strengthened or weakened interaction on reduced surface compared with stoichiometric surface are related to a different amount of electron transfer and a variation of chemical bonding with TM sp-Ti $3d$ bonding at O_v site.

Our complete study of the diffusion barrier is useful for the design and synthesis of the bimetallic clusters which generally exhibit better catalytic activity and thermal stability[145] than monophase clusters. A series of bimetallic clusters such as Ni-Au[106], Pt-Au[147,148], Pt-Rh[149], Pd-Au,[150] Pt-Co[151], and Co-Ni[152] have been synthesized on TiO_2 surface. It has been pointed out that multicomponent clusters can only be synthesized with a proper deposition sequence: growing TM species with less mobility first and depositing TM atoms with higher mobility next.[106,148] Thus the knowledge of the relative mobility between the involved TM adatoms is important for the synthesis and the understanding of the sintering mechanism for bimetallic clusters. Most of the bimetallic clusters synthesized so far are taken on the stoichiometric surface, however, to take advantage of the O_v defect for activating the clusters, bimetallic clusters synthesized on reduced surface are highly desired. However, O_v effect on the TM diffusion has been less studied. Since the adsorption and diffusion of TM adatoms are affected by the content of free charge carriers (electron/hole) on the surface, it should be noted that the diffusion barrier

also changes accordingly depending on the O_v content on the surface. Nevertheless, our study still provides a direct evaluation of the O_v's effect on the diffusion of the chosen TM species and guidelines the synthesis of multi-component clusters with different combination possibilities of the involved TM species.

C. Ti^{3+} States Related to TM Adsorption

Depending on the strength of interfacial reaction, adsorption of TM clusters on the oxide surface can induce an oxidation of interfacial TM atoms or a reduction of cation ions of the support.[153] A strong interaction may induce the formation of Ti^{3+} gap states which are overlapped with the O_v induced Ti^{3+} states in XPS spectra.[32] From application side, it is very important to determine the oxidation state of the TM adatoms and consider the possibility of the reduction of the surface through detecting the in-gap Ti^{3+} states. However, experimentally observed peaks related to the gap states can be either characteristics of deposited metal states[74] or Ti^{3+} states due to redox reaction between deposited TM atoms and oxide ions[108] or Ti^{3+} states related to the O_v on the surface.[32] The assignment of the origin of the states for several TM overlayers is still subject to debate.[32,33] For Fe, Co and Ni adsorbed on stoichiometric surface, the in-gap states are widely recorded.[32,74,101,108] Diebold found that the gap states due to Fe adsorption appear at exactly the same energy position as gap states induced by removal of surface oxygen and proposed that it arises from a position change of bridging oxygen atoms upon Fe adsorption.[32] Our calculation shows that, for Fe, Co and Ni adatom on stoichiometric surface, there is no in-gap states near the bottom of conduction band and thus excluding the possibility of Ti reduction due to charge transfer. However, as significant amounts of electron are found to be transferred from VIIIB adatoms to *s*-TiO_2 surface and strongly polaronic effects exist on the TiO_2 surface, at finite temperature, the reduction of Ti ions may still occur due to a combined effect of the charge transfer and the interfacial oxygen displacement.

In contrast to the possible introduction of Ti^{3+} states by TM adsorption on stoichiometric surface, for TM clusters adsorbed on reduced surface, the defective Ti^{3+} states can be quenched when the excess electrons distributed on the reduced Ti site are transferred to the TM adsorbates. This phenomenon is more likely to appear for those TM species with large electronegativity like Pt and Rh. Indeed, studies have shown that the original Ti^{3+} defective states vanish completely after evaporation of small amounts of Pt on the surface.[133–135] However, the effects of Pt on the variation of Ti^{3+} states is more complex as experimental studies have indicated that adsorption of Pt also decreases the formation energy of O_v and promotes the formation of O_v and Ti^{3+} states on the surface.[130]

The spatial localization of the Ti^{3+} defective states has been intensively studied.[36] While earlier studies have shown that the two excess electrons are mainly localized on the adjacent Ti_{6c}(d) atoms around O_v site, our present study shows that only about 5% of the excess electrons are distributed on the surface and occupy the Ti_{5c1}(d) and Ti_{5c2}(d) sites and no electron is found at the Ti_{6c}(d) site. Our result is consistent with the recent occupied-state STM and STS measurements with an atomic-scale resolution which find four bright lobes around each O_v center corresponding to the distribution of excess electrons occupying at the Ti_{5c} sites.[48] Low temperature STM measurement shows that these Ti_{5c} sites are the main adsorption sites for CO rather than the O_v site.[45] Moreover, the O_2 molecule, as a common electron scavenger over TiO_2 that can take up electrons from the surface,[154] has been shown to be able to adsorb and dissociate at the Ti_{5c} sites without a direct interaction with O_v center, which again suggests a locally electron-rich environment at these Ti_{5c} sites.[46] It is expected that these excess electrons at Ti_{5c} sites may transfer to some strongly electronegative species as O_2 on the surface. Indeed, our calculation of the PESs for Au and Pt shows a local minimum at the Ti_{5c} site, which is absent for other less electronegative TM species like Ag and Cu, suggesting a moderate electron transfer and chemical interaction at this site.

It is highly interesting to investigate the effect of deposition of TM species on the redistribution of these Ti^{3+} defective states around the O_v center. It is widely accepted that the perimeter interface[49–51] serves as an important site for anchoring and activating the reactant and intermediate products during catalytic processes. A plausible reason is that there are some excess electrons accumulating at these perimeter sites and creating a locally electron-rich environment. To confirm this hypothesis, we investigate the variation of the distribution of excess electrons on the Ti_{5c} sites upon decorating different TM monomers. We calculate the amounts of excess electrons localized at the Ti_{5c1}(d) and Ti_{5c2}(d) sites by integrating the LDOS of the Ti atoms in the band-gap region. Fig. 14 shows the amounts of excess electrons on both sites subtracted by the corresponding values of pristine reduced surface. For all the cases, there is an increase in the amounts of excess electrons localized on the Ti_{5c} sites near the TM adsorption site. The amounts of excess electrons on the Ti_{5c1}(d) site for Au, Ag, Cu, and Pd cases remain nearly the same as those on pristine surface. A clear enhancement of electron accumulation is shown at the Ti_{5c2}(d) site for most of the TM species except Pd. Due to a small electronegativity, Fe monomer even donates some electrons to the reduced surface thus inducing the largest population at Ti_{5c1}(d) site. For Au and Pt which take up significant electrons from the surface due to a large electronegativity, the surprisingly enhancement of excess electrons around the Ti_{5c} site suggests that the accumulated electrons on the TM monomers are mainly from the excess electrons initially located at subsurface. The enhanced accumulation of the

excess electrons around the perimeter may be the underlying reason for the promoted activity commonly found in these deposited clusters.

V. CONCLUSIONS

Size and thermal stability are two important indicators for most of the supported clusters for a variety of applications. Both of them are closely related to the interfacial interaction between TM species and the support during growth and applications. In this study, we perform a systematic DFT study of the adsorption and diffusion of different TM monomers on both stoichiometric and reduced TiO_2 (110) surface. In contrast to the general belief that the presence of O_v enhances the binding of TM on the surface, we find that O_v can weaken the interaction and enhance the diffusion for Fe, Co, Ni, Ag, and Cu adatoms.

Our hybrid functional calculation allows an accurate description of the alignment of the orbitals of TM adatoms with the band gap of the surface and the degree of charge transfer between the TM adatoms and the surface. For the pristine reduced surface, the excess electrons induce Ti^{3+} reduced states. Only a small portion (around 5%) of these excess electrons distribute on the topmost surface, and the excess electrons on the top layer are further found to be primarily localized on the Ti_{5c} atoms on the basal plane outside the O_v. The small amounts of excess electrons populating at these Ti_{5c} sites can be transferred to strongly electronegative adsorbates like Au and Pt thus enabling a moderate adsorption as reflected in the metastable adsorption at Ti_{5c} sites in the PES plots, whereas similar charge transfer and stable adsorption are absent for other less electronegative TM adatoms and for adsorption on stoichiometric surface. This indicates that the excess electrons should affect chemical reactivity of reduced TiO_2 (110) surfaces. The excess electrons localized at the Ti_{5c} sites should attract the electron scavengers like O_2 and CO, and repel the less electronegative H_2O and NH_3 molecules. Indeed, low temperature measurements show that the Ti_{5c} sites are the main adsorption sites for CO molecule[45] and the accumulated excess electrons at these sites even enable a dissociative adsorption of O_2 without a direct interaction with O_v.[46]

With the accompanying excess electrons, the presence of O_v on the surface makes most of the TM monomers negatively charged. On the other hand, the presence of TM species on the O_v site triggers a redistribution of the excess electrons on the surface. It is believed that the significant amount of excess electrons initially distributed at the subsurface of the pristine surface without adsorbates are "pumped out" to the topmost surface after TM adsorption and partially transferred to the TM adatoms. The amounts of excess electrons located on the Ti_{5c} atoms near the perimeter interface increases accordingly. This may explain the critical role of the perimeter interface in activating the adsorbed reactants for a variety of reactions.

[1] Weiher, N.; Bus, E.; L. Delannoy; Louis, C.; Ramaker, D. E.; Miller, J. T.;van Bokhoven, J. A. J. Catal. 2006, 240, 100.

[2] Kundu, S.; Ciston, J.; Senanayake, S. D.; Arena, D. A.; Fujita, E.; Stacchiola, D.; Barrio, L.; Navarro, R. M.; G. Fierro, J. L.; Rodriguez, J. A. J. Phys. Chem. C 2012, 116, 14062.

[3] Taing, J.; Cheng, M. H.; Hemminger, J. C. ACS Nano, 2011, 5, 6325.

[4] Muhich, C. L.; Zhou, Y.; Holder, A. M.; Weimer, A. W.; Musgrave, C. B. J. Phys. Chem. C 2012, 116, 10138.

[5] Nishikawa, M.; Mitani, Y.; Nosaka, Y. J. Phys. Chem. C 2012, 116, 14900.

[6] An, W. -J.; Wang, W. -N.; Ramalingam, B.; Mukherjee, S.; Daubayev, B.; Gangopadhyay, S.; Biswas, P. Langmuir 2012, 28, 7528.

[7] Ren Su,; Tiruvalam, R.; He, Q.; Dimitratos, N.; Kesavan, L.; Hammond, C.; Lopez-Sanchez, J. A.; Bechstein, R.; Kiely, C, J.; Hutchings, G. J.; Besenbacher, F. ACS Nano 2012, 6, 6284.

[8] Mitsuhara, K.; Tagami, M.; Matsuda, T.; Visikovskiy, A.; Takizawa, M.; Kido, Y. J. Chem. Phys. 2012, 136, 124303.

[9] Newton, M. A.; Belver-Coldeira, C.; Martínez-Arias, A.; Fernández-García M. Nature Materials 2007, 6, 528.

[10] M. Ni,; Leung, M. K. H.; Leung, D. Y. C.; Sumathy, K. Renewable and Sustainable Energy Reviews 2007, 11, 401.

[11] Wang, W.-N.; An, W.-J.; Ramalingam, B.; Mukherjee, S.; Niedzwiedzki, D. M.; Gangopadhyay, S.; Biswas, P. J. Am. Chem. Soc. 2012, 134, 11276.

[12] Shekhar, M.; Wang, J.; Lee, W.-S.; Williams, W. D.; Kim, S. M.; Stach, E. A.; Miller, J. T.; Delgass, W. N.; Ribeiro, F. H. J. Am. Chem. Soc. 2012, 134, 4700.

[13] Valden, M.; Lai, X.; Goodman, D. W. Science 1998, 281, 1647.

[14] Haruta, M.; Kobayashi, T.; Sano, H.; Yamada, N. Chem. Lett. 1987, 2, 405.

[15] Kaden, W. E.; Wu, T.; Kunkel, W. A.; Anderson, S. L. Science 2009, 326, 826.

[16] Hansen, J. ø.; Lira, E.; Galliker, P.; Wang, J.-G.; Sprunger, P. T.; Li, Z.; Lægsgaard, E.; Wendt,S.; Hammer,B.; Besenbacher, F. J. Phys. Chem. C 2010, 114, 16964.

[17] Diebold, U.; Pan, J.-M.; Madey, T. E. Phys. Rev. B 1993, 47, 3868.

[18] Sedona, F.; Sambi, M.; Artiglia, L.; Rizzi, G. A.; Vittadini, A.; Fortunelli, A.; Granozzi, G. J. Phys. Chem. C, 2008, 112, 3187.

[19] Zanella, R.; Rodríguez-González, V.; Arzola, Y.; Moreno-Rodriguez, A. ACS Catal. 2012, 2, 1.

[20] Negra, M. D.; Nicolaisen, N. M.; Li, Z.; Møller, P. J. Surf. Sci. 2003, 540, 117.

[21] Ono, L. K.; Yuan, B.; Heinrich, H.; Cuenya, B. R. J. Phys. Chem. C 2010, 114, 22119.

[22] Diebold, U. Surface Science Reports 2003, 48, 53.

[23] Dohnálek, Z.; Lyubinetsky, I.; Rousseau, R. Progress in Surface Science 2010, 85, 161.
[24] Cuenya, B. R. Thin Solid Films 2010, 518, 3127.
[25] Behafarid, F.; Roldan Cuenya, B. Surf. Sci. 2012, 606, 908.
[26] Ruckenstein, E.; Dadyburjor, D. B Reviews in Chemical Engineering, 2011, 1, 251.
[27] Kartusch, C.; Krumeich, F.; Safonova, O.; Hartfelder, U.; Makosch, M.; Sá, J.; van Bokhoven, J. A. ACS Catal. 2012, 2, 1394.
[28] Sá, J.; Taylor, S. F. R.; Daly, H.; Goguet, A.; Tiruvalam, R.; He, Q.; Kiely, C. J.; Hutchings, G. J.; Hardacre, C. ACS Catal. 2012, 2, 552.
[29] Zhang, Z.; Tang, W.; Neurock, M.; Yates, J. T. Jr. J. Phys. Chem. C 2011, 115, 23848.
[30] Fu, Q.; T. Wagner, Surface Science Reports 2007, 62, 431.
[31] Awate, S. V.; Deshpande, S. S.; Rakesh, K.; Dhanasekaran, P.; Gupta, N. M. Phys. Chem. Chem. Phys., 2011, 13, 11329.
[32] Diebold, U.; Tao, H.-S.; Shinn, N. D.; Madey, T. E. Phys. Rev. B 1994, 50, 14474.
[33] Nakajima, N.; Kato, H.; Okazaki, T.; Sakisaka, Y. Surf. Sci., 2004, 561, 93.
[34] Teoh, W. Y.; Mäller, L.; Amal, R. J. Catal. 2007, 251, 271.
[35] Yoon, B.; Häkkinen, H.; Landman, U.; Wörz, A. S.; Antonietti, J.-M.; Abbet, S.; Judai, K.; Heiz, U. Science, 2005, 307, 403.
[36] Connelly, K. A.; Idriss, H. Green Chem., 2012, 14, 260.
[37] Yim, C. M.; Pang, C. L.; Thornton, G. Phys. Rev. Lett. 2010, 104, 036806.
[38] Kowalski, P. M.; Camellone, M. F.; Nair, N. N.; Meyer, B.; Marx, D. Phys. Rev. Lett. 2010, 105, 146405.
[39] Zhang, Z.; Jeng, S.-P.; Henrich, V. E. Phys. Rev. B 1991, 43, 12004.
[40] Lindan, P. J. D.; Harrison, N. M.; Gillan, M. J.; White, J. A. Phys. Rev. B 1997, 55, 919.
[41] Chrétien, S.; Metiu, H. J. Phys. Chem. C 2011, 115, 4696.
[42] Di Valentin, C.; Pacchioni, G.; Selloni, A. Phys. Rev. Lett. 2006, 97, 166803.
[43] Ke, Q.; Lou, X.; Wang, Y.; Wang, J. Phys. Rev. B 2010, 82, 024102.
[44] Ke, Q.; Kumar, A.; Lou, X.; Zeng, K.; Wang, J. Appl. Phys. Lett. 2012, 100, 042902.
[45] Zhao, Y.; Wang, Z.; Cui, X. F.; Huang, T.; Wang, B.; Luo, Y.; Yang, J. L.; Hou, J. G. J. Am. Chem. Soc. 2009, 131, 7958.
[46] RWendt, S.; Sprunger, P. T.; Lira, E.; Madsen, G. K. H.; Li, Z. S.; Hansen, J. O.; Matthiesen, J.; Blekinge-Rasmussen, A.; Laegsgaard, E.; Hammer, B.; Besenbacher, F. Science, 2008, 320, 1755.
[47] Wang, Z.-T.; Du, Y.; Dohn alek, Z.; Lyubinetsky, I. J. Phys. Chem. Lett. 2012, 1, 3524.
[48] Minato, T.; Sainoo, Y.; Kim, Y.; Kato, H. S.; Aika, K.; Kawai, M.; Zhao, J.; Petek, H.; Huang, T.; He, W.; Wang, B.; Wang, Z.; Zhao, Y.; Yang, J. L.; Hou, J. G. J. Chem. Phys. 2009, 130, 124502.
[49] Haruta, M. Bulletin G. 2004, 37, 1. (need check)
[50] Panayotov, D. A.; Burrows, S. P.; John T. Yates, Jr.; Morris, J. R. J. Phys. Chem. C 2011, 115, 22400.
[51] Green, I. X.; Tang, W.; McEntee, M.; Neurock, M.; John T. Yates, Jr. J. Am. Chem. Soc. 2012, 134, 12717.
[52] Giordano, L.; Pacchioni, G.; Bredow, T.; Sanz, J. F. Surf. Sci. 2001, 471, 21.
[53] Vijay, A.; Mills, G.; Metiu, H. J. Chem. Phys. 2003, 118, 6536.
[54] Matthey, D.; Wang, J. G.; Wendt, S.; Matthiesen, J.; Schaub, R.; Lægsgaard, E.; Hammer, B.; Besenbacher, F. Science 2007, 315.
[55] Rasmussen, M. D.; Molina, L. M.; Hammer, B. J. Chem. Phys. 2004, 120, 988.
[56] Kresse, G.; Furthmüller, Phys. Rev. B 1996, 54, 11169.
[57] Perdew, J.; Burke, K.; Ernzerhof, M. Phys. Rev. Lett. 1996, 77, 3865.
[58] Heyd, J.; Scuseria, G. E.; Ernzerhof, M. J. Chem. Phys. 2003, 118, 8207.
[59] Gai, Y. Q.; Li, J. B.; Li, A. S.; Xia, J. B.; Wei, S. H. Phys. Rev. Lett. 2009, 102, 036402.
[60] Zhang, Z.; Jeng, S.-P.; Henrich, V. E. Phys. Rev. B 1991, 43, 12004.
[61] Krüger, P.; Jupille, J.; Bourgeois, S.; Domenichini, B.; Verdini, A.; Floreano, L.; Morgante, A. Phys. Rev. Lett. 2012, 108, 126803.
[62] Calzado, C. J.; Hernández, N. C.; Sanz, J. F. Phys. Rev. B 2008, 77, 045118.
[63] Kruger, P.; Bourgeois, S.; Domenichini, B.; Magnan, H.; Chandesris, D.; Le Fevre, P.; Flank, A. M.; Jupille, J.; Floreano, L.; Cossaro, A.; Verdini, A.; Morgante, A. Phys. Rev. Lett. 2008, 100, 055501.(check author)
[64] Camellone, M. F.; Kowalski, P. M.; Marx, D. Phys. Rev. B 2011, 84, 035413.
[65] Deskins, N. A.; Rousseau, R.; Dupuis, M. J. Phys. Chem. C 2011, 115, 7562.
[66] Yang, S.; Halliburton, L. E.; Manivannan, A.; Bunton, P. H.; Baker, D. B.; Klemm, M.; Horn, S.; Fujishima, A. Appl. Phys. Lett 2009, 94, 162114.
[67] Anthoula C. Papageorgiou, C. L. P. G. T. G. C. Q. C. A. J. F.W. A. H., Nikolaos S. Beglitis; Thornton, G. Proc. Natl. Acad. Sci. U.S.A. 2009, 107, 2391.
[68] Zhang, J.; Alexandrova, A. N. J. Chem. Phys. 2011, 135, 174702.
[69] Charlton, G.; Howes, P. B.; Muryn, C. A.; Raza, H.; Jones, N.; Taylor, J. S. G.; Norris, C.; McGrath, R.; Norman, D.; Turner, T. S.; Thornton, G. Phys. Rev. B 2000, 61, 16117.
[70] Sieberer, M.; Redinger, J.; Mohn, P. Phys. Rev. B 2007, 75, 035203.
[71] Chun, W.-J.; Koike, Y.; Ijima, K.; Fujikawa, K.; Ashima, H.; Nomura, M.; Iwasawa, Y.; Asakura, K. Chem. Phys. Lett. 2007, 433, 345.
[72] Tanizawa, Y.; Shido, T.; Chun, W.-J.; Asakura, K.; Nomura, M.; Iwasawa, Y. J. Phys. Chem. B 2003, 107, 12917.
[73] Anastasopoulos, A.; Hayden, B. E. Surf. Sci. 2011, 605, 174.
[74] See, A. K.; Bartynski, R. A. Phys. Rev. B 1994, 50, 12064.
[75] Tong, X.; Benz, L.; Chrétien, S.; Kemper, P.; Kolmakov, A.; Metiu, H.; Bowers, M. T.; Buratto, S. K. J. Chem. Phys. 2005, 123, 204701.
[76] Tong, X.; Benz, L.; Kolmakov, A.; Chrétien, S.; Metiu, H.; Buratto, S. K. Surf. Sci. 2005, 575, 60.
[77] Sivaramakrishnan, S.; Tedjasaputra, A. P.; Sato, K.; Zuo J. M. J. Appl. Phys. 2010, 107, 053505.
[78] Ma, Z.; Dai, S. ACS Catal. 2011, 1, 805.
[79] Tong, X.; Benz, L.; Chréien, S.; Metiu, H.; Bowers, M. T.; Buratto, S. K. J. Phys. Chem. C 2010, 114, 3987.
[80] Chen, M.; Wayne Goodman, D. Chem. Soc. Rev. 2008, 37, 1860.
[81] Schwartz, V.; Mullins, D. R.; Yan, W.; Chen, B.; Dai, S.;

Overbury, S. H. J. Phys. Chem. B 2004, 108, 15782.
[82] Lopez, N.; Nøskov, J. K. Surf. Sci. 2002, 515, 175.
[83] Wahlstro, E.; Lopez, N.; Schaub, R.; Thostrup, P.; Rønau, A.; Africh, C.; Lægsgaard, E.; Nøskov, J. K.; Besenbacher, F. Phys. Rev. Lett. 2003, 90, 026101.
[84] Pillay, D.; Hwang, G. S. Phys. Rev. B 2005, 72, 205422.
[85] Pabisiak T.; Kiejna, A. Phys. Rev. B 2009, 79, 085411.
[86] Pabisiak, T.; Kiejna, A. Surf. Sci. 2011, 605, 668.
[87] Goldman, N.; Browning, N. D. J. Phys. Chem. C 2011, 115, 11611.
[88] Tong, X.; Benz, L.; Kemper, P.; Metiu, H.; Bowers, M. T.; Buratto, S. K. J. Am. Chem. Soc. 2005, 127, 13516.
[89] Okazawa, T.; Fujiwara, M.; Nishimura, T.; Akita, T.; Kohyama, M.; Kido, Y. Surf. Sci. 2006, 600, 1331.
[90] Okazawa, T.; Kohyama, M.; Kido, Y. Surf. Sci. 2006, 600, 4430.
[91] Chung, H. J.; Yurtsever, A.; Sugimoto, Y.; Abe, M.; Morita, S. Appl. Phys. Lett. 2011, 99, 123102.
[92] Jiang, Z.; Zhang, W.; Jin, L.; Yang, X.; Xu, F.; Zhu, J.; Huang, W. J. Phys. Chem. C, 2007, 111, 12434.
[93] Zhang, L.; Persaud, R.; Madey, T. E. Phys. Rev. B 1997, 56, 10549.
[94] Wörz, A. S.; Heiz, U.; Cinquini, F.; Pacchioni, G. J. Phys. Chem. B 2005, 109, 18418.
[95] Kruse, N.; Chenakin, S. Applied Catalysis A: General 2011, 391, 367.
[96] Chen, M.; Cai, Y.; Yan, Z.; Goodman, D. W. J. Am. Chem. Soc. 2006, 128, 6341.
[97] Willneff, E. A.; S. Braun,; Rosenthal, D.; Bluhm,H.; Häecker, M.; Kleimenov, E.; Knop-Gericke, A.; Schlögl, R.; Schroeder, S. L. M. J. Am. Chem. Soc. 2006, 128, 12052.
[98] Chen, C. S.; Chen, T. C.; Chen, C. C.; Lai, Y. T.; You, J. H.; Chou, T. M.; Chen, C. H.; Lee, J.-F. Langmuir 2012, 28, 9996.
[99] Pan, J.-M.; Madey, T. E. J. Vac. Sci. Technol. A 1993, 11, 1667.
[100] Mostéfa-Sba, H.; Domenichini, B.; Bourgeois, S. Surf. Sci. 1999, 437, 107.
[101] Nakajima, N.; Kato, H.; Okazaki, T.; Sakisaka, Y. Surf. Sci. 2004, 561, 79.
[102] Tohji, K.; Udagawa, Y.; Tanabe, S.; Ida, T.; Ueno, A. J. Am. Chem. Soc. 1984, 106, 5172.
[103] Shao, Y.; Chen, W.; Wold, E.; Paul, J. Langmuir 1994, 10, 178.
[104] Ding, B.; Cheng, F.; Pan, F.; Fa, T.; Yao, S.; Potzger, K.; Zhou, S. Journal of Magnetism and Magnetic Materials 2012, 324, 33.
[105] Fujikawa, K.; Suzuki, S.; Koike, Y.; Chun, W.-J.; Asakura, K. Surf. Sci. 2006, 600, L117.
[106] Tenney, S. A.; He, W.; Roberts, C. C.; Ratliff, J. S.; Shah, S. I.; Shafai, G. S.; Turkowski, V.; Rahman, T. S.; Chen, D. A. J. Phys. Chem. C 2011, 115, 11112.
[107] Onishi, H.; Aruga, T.; Egawa, C.; Iwasawa, Y. Surf. Sci. 1990, 233, 261.
[108] Domenichinia, B.; Šutara, F.; Škála, T.; Matolín, V.; Bourgeois, S. Journal of Electron Spectroscopy and Related Phenomena 2011, 184, 410.
[109] Pan, J. S.; Tao, J. G.; Huan, H. A.; Chiam, S. Y.; Zhang, Z.; Li, D. T. H.; Sun, Y.; Chai, J. W.; Wang S. J.; Sun, C. Q. Surf. Interface Anal. 2010, 42, 878.
[110] Espinós, J. P.; González-Elipe, A. R.; Caballero, A.; García, J.; Munuera, G. J. Catal. 1992, 136, 415.
[111] Aizawa, M.; Lee, S.; Anderson, S. L. J. Chem. Phys. 2002, 117, 5001.
[112] Koike, Y.; Ijima, K.; Chun, W.-J.; Ashima, H.; Yamamoto, T.; Fujikawa, K.; Suzuki, S.; Iwasawa, Y.; Nomura, M.; Asakura, K. Chem. Phys. Lett. 2006, 421, 27.
[113] Sasahara, A.; Hiehata, K.; Onishi, H. Catal Surv Asia 2009, 13, 9.
[114] Fu, Q.; Wagner, T.; Olliges, S.; Carstanjen, H.-D. J. Phys. Chem. B 2005, 109, 944.
[115] Bonanni, S.; Aït-Mansour, K.; Brune, H.; Harbich, W. ACS Catal. 2011, 1, 385.
[116] Murugan, P.; Kumar, V.; Kawazoe, Y. Phys. Rev. B 2006, 73, 075401.
[117] Xu, C.; Lai, X.; Zajac, G. W.; Goodman, D. W. Phys. Rev. B 1997, 56, 13464.
[118] San-Miguel, M. A.; Oviedo, J.; Sanz, J. F. Phys. Rev. B 2007, 99, 066102.
[119] Jak, M. J. J.; Konstapel, C.; van Kreuningen, A.; Verhoeven, J.; Frenken, J. W. M. Surf. Sci. 2000, 457, 295.
[120] Sanz, J. F.; Márquez, A. J. Phys. Chem. C 2007, 111, 3949.
[121] Ong, S. V.; Khanna, S. N. J. Phys. Chem. C 2011, 115, 20217.
[122] Jaka, M. J. J.; Konstapela, C.; van Kreuningena, A.; Chrosta, J.; Verhoevena, J.; Frenken, J. W. M. Surf. Sci. 2001, 474, 28.
[123] Watanabe, Y.; Wu, X.; Hirata, H.; Isomura, N. Catal. Sci. Technol. 2011, 1, 1490.
[124] Dulub, O.; Hebenstreit, W.; Diebold, U. Phys. Rev. Lett. 2000, 84, 3646.
[125] Naitabdi, A.; Behafarid, F.; Roldan Cuenya, B. Appl. Phys. Lett. 2009, 94, 083102.
[126] Iddir, H.; Öğüt, S.; Browning, N. D.; Disko, M. M. Phys. Rev. B 2005, 72, 081407(R).
[127] Iddir, H.; Skavysh, V.; Öğüt, S.; Browning, N. D.; Disko, M. M. Phys. Rev. B 2006, 73, 041403(R).
[128] Çelik, V.; Ünal, H.; Mete, E.; Ellialtioğlu, Ş. Phys. Rev. B 2010, 82, 205113.
[129] Yongprapat, S.; Therdthianwong, S.; Kritayakornupong, C.; Computational Materials Science 2008, 44, 536.
[130] Ammal, S. C.; Heyden, A. J. Phys. Chem. C 2011, 115, 19246.
[131] Sasahara, A.; Pang, C. L.; Onishi, H. J. Phys. Chem. B 2006, 110, 13453.
[132] Sasahara, A.; Hiehata, K.; Onishi, H.; Catal Surv Asia 2009, 13, 9.
[133] Fischera, S.; Martín-Gago, J. A.; Romáb, E.; Schierbaum, K. D.; de Segovia J. L., Journal of Electron Spectroscopy and Related Phenomena 1997, 83, 217.
[134] Fischer, S.; Schneiderb, F.; Schierbaum, K.-D. Vacuum 1996, 47, 1149.
[135] Schierbaum, K. D.; Fischer, S.; Torquemada, M. C.; de Segovia, J. L.; Romám, E.; Martín-Gago, J. A. Surf. Sci. 1996, 345, 261.
[136] Gana, S.; Liang, Y.; Baer, D. R.; Grant, A. W. Surf. Sci. 2001, 475, 159.
[137] Schierbaum, K. D.; Fischer, S.; Torquemada, M. C.; de Segovia, J. L.; Romám, E.; Martín-Gago, J. A. Surf. Sci. 345, 1996, 261.
[138] Bonanni, S.; Aït-Mansour, K.; Harbich, W.; Brune, H. J. Am. Chem. Soc. 2012, 134, 3445.
[139] Deskins, N. A.; Rousseau, R.; Dupuis, M. J. Phys. Chem. C 2010, 114, 5891.
[140] Kimura, K.; Naya, S.-i.; Jin-nouchi, Y.; Tada, H. J. Phys.

Chem. C 2012, 116, 7111.
[141] Cai, Y.; Zhang, A.; Feng, Y. P.; Zhang, C.; Teoh, H. F.; Ho, G. W. J. Chem. Phys. 2009, 131, 224701.
[142] Cai, Y.; Zhou, M,; Zeng, M.; Zhang, C.; Feng, Y. P. Nanotechnology 2011, 22, 215702.
[143] Panayotov, D. A.; Burrows, S. P.; Jr.,J. T. Yates; Morris, J. R. J. Phys. Chem. C 2011, 115, 22400
[144] Martinez, U.; Hammer, B. J. Chem. Phys. 2011, 134, 194703.
[145] Kaden, W. E.; Tianpin Wu,; Kunkel, W. A.; Anderson, S. L. Science 2007, 315.
[146] Zhou, J.; Kang, Y. C.; Chen, D. A. Surf. Sci. 2003, 537, L429.
[147] Tenney, S. A.; Ratliff, J. S.; Roberts, C. C.; He, W.; Ammal, S. C.; Heyden, A.; Chen, D. A. J. Phys. Chem. C 2010, 114, 21652.
[148] Park, J. B.; Conner, S. F.; Chen, D. A. J. Phys. Chem. C 2008, 112, 5490.
[149] Ozturk, O.; Park, J. B.; Ma, S.; Ratliff, J. S.; Zhou, J.; Mullins, D. R.; Chen, D. A. Surf. Sci. 2007, 601, 3099.
[150] Han, P.; Goodman, D. W. J. Phys. Chem. C 2008, 112, 6390.
[151] Papaefthimiou, V.; Dintzer, T.; Lebedeva, M.; Teschner, D.; Hävecker, M.; Knop-Gericke, A.; Schlögl, R.; Pierron-Bohnes, V.; Savinova, E.; Zafeiratos, S. J. Phys. Chem. C 2012, 116, 14342.
[152] Takanabe, K.; Nagaoka, K.; Nariai, K.; Aika, K.-i. J. Catal. 2005, 232, 268.
[153] Nolan, M. J. Chem. Phys. 2012, 136, 134703.
[154] Petrik, N. G.; Kimmel, G. A. J. Phys. Chem. C 2011, 115, 152.

TABLE I: Adsorption properties of TM adatoms on stoichiometric TiO_2 (110) surface. E_b: binding energy; CN: coordination number; r: bond length, where there are several TM-O bonds, we report only the range of lengths; δQ(e): the charge transfer from TM adatoms to the surface, a positive (negative) value means a positively (negatively) charged state of TM on the surface.

	site	E_b(eV)	CN	r(TM-O)(Å)	$\delta Q(e)$
Au	O_{2c}	1.02	1	1.98	0.63
Ag	B_o	1.72	2	2.26	0.78
Cu	B_o	2.75	2	1.86	0.80
Fe	T_1	4.54	3	1.84-1.93	1.48
Co	T_1	4.01	3	1.83-1.98	1.37
Ni	B_o	3.71	2	1.81	0.85
Pd	B_o	1.94	2	2.08	0.72
Pt	B_o	2.66	2	1.93	0.64
	T_2	2.59	2	2.02	0.11

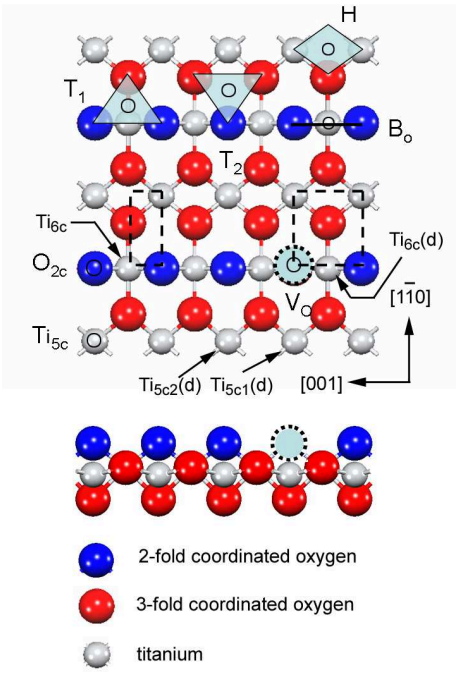

FIG. 1: Atomic model of the TiO_2 (110) surface with the (4 × 2) supercell: top view (top) and side view (bottom). Possible adatom adsorption sites on the stoichiometric surface are labeled and shown by small circles. The bridging oxygen vacancy on the reduced surface is represented by a dashed circle. The small (large) dashed rectangle represents the region in the s-TiO_2 (r-TiO_2) surface for which the diffusion profiles of the TM adatoms on the surface are calculated.

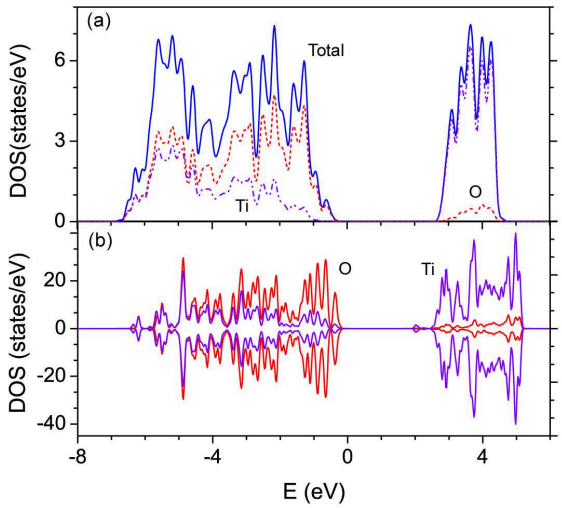

FIG. 2: (a)DOS of bulk rutile TiO_2; (b) LDOS of atoms in the topmost O-Ti_2O_2-O layer of s-TiO_2 (110) surface by hybrid functional calculation.

TABLE II: Adsorption properties of TM adatoms on reduced TiO_2 (110) surface. E_b: binding energy; CN: coordination number; r: bond length, where there are several TM-Ti bonds, we report only the range of lengths; δQ(e): the charge transfer from TM adatoms to the surface, a positive (negative) value means a positively (negatively) charged state of TM on the surface.

	Site	E_b(eV)	CN	r(TM-Ti)(Å)	$\delta Q(e)$
Au	O_v	2.55	2	2.62	-0.51
	Ti_{5c}	1.28	1	2.44	
Ag	O_v	1.37	2	2.75	-0.24
Cu	O_v	1.92	2	2.54	-0.30
Fe	O_v	2.57	5	2.48-2.63	0.43
Co	O_v	2.86	5	2.47-2.61	-0.01
Ni	O_v	2.93	2	2.27	-0.52
Pd	O_v	2.41	2	2.41	-0.30
Pt	O_v	4.64	2	2.36	-0.96
	Ti_{5c}	2.90	1	2.13	

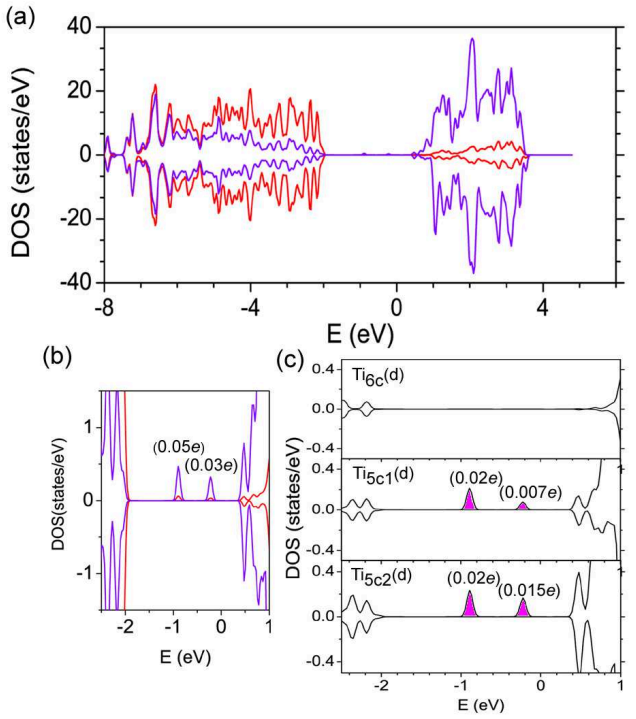

FIG. 3: (a)LDOS of atoms in the topmost O-Ti_2O_2-O layer of r-TiO_2 (110) surface. (b) Enlarged view of (a) to show the defective state in the band gap for r-TiO_2 (110) surface. (c) LDOS of the adjacent fivefold coordinated Ti atoms around the O_v. Electronic populations of the defective levels (shadow area) are labeled.

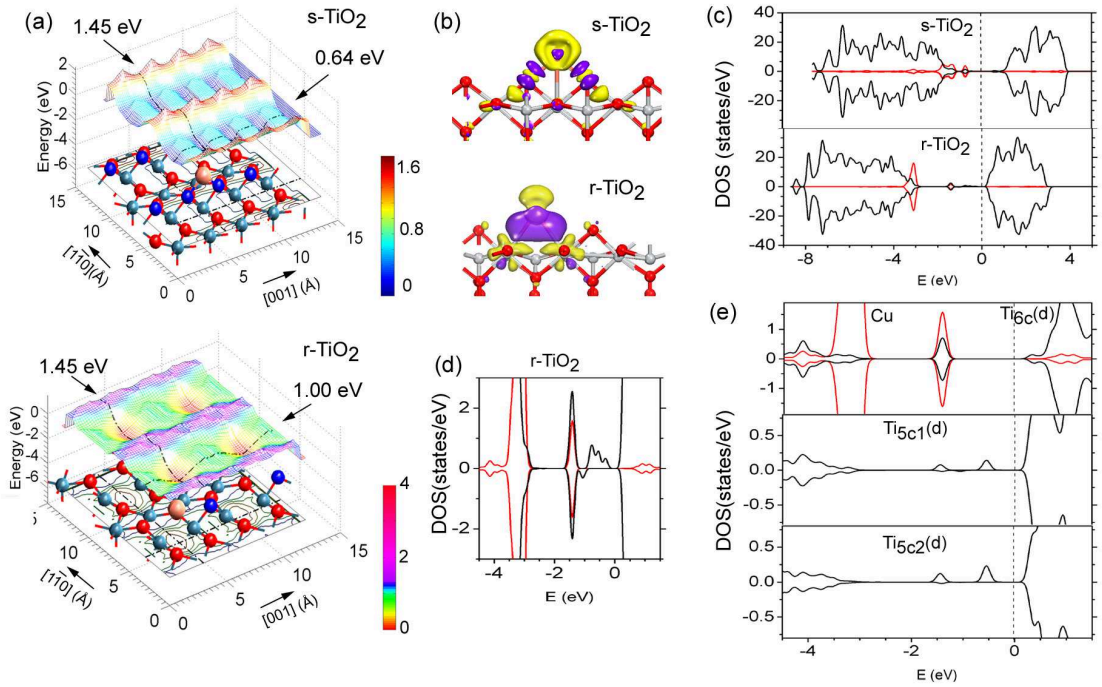

FIG. 4: (a)PES for Cu diffusing on *s*-/*r*- TiO_2 surfaces. Activation barriers are labeled for Cu hopping between the minimums along [001] and [110] directions (dashed lines). The spheres in red, blue, and violet color represent O_{2c}, O_{3c}, Ti atoms respectively. (b)Isosurface of the differential charge density, yellow (purple) color denotes diminishing (accumulation) of electrons. (c)LDOS of atoms at the topmost O-Ti_2O_2-O layer calculated from configuration of the most stable adsorption. (d) Enlarged view of (c). (e) LDOS of the adjacent fivefold coordinated Ti atoms around the O_v after Ag adsorption on the *r*-TiO_2 surface.

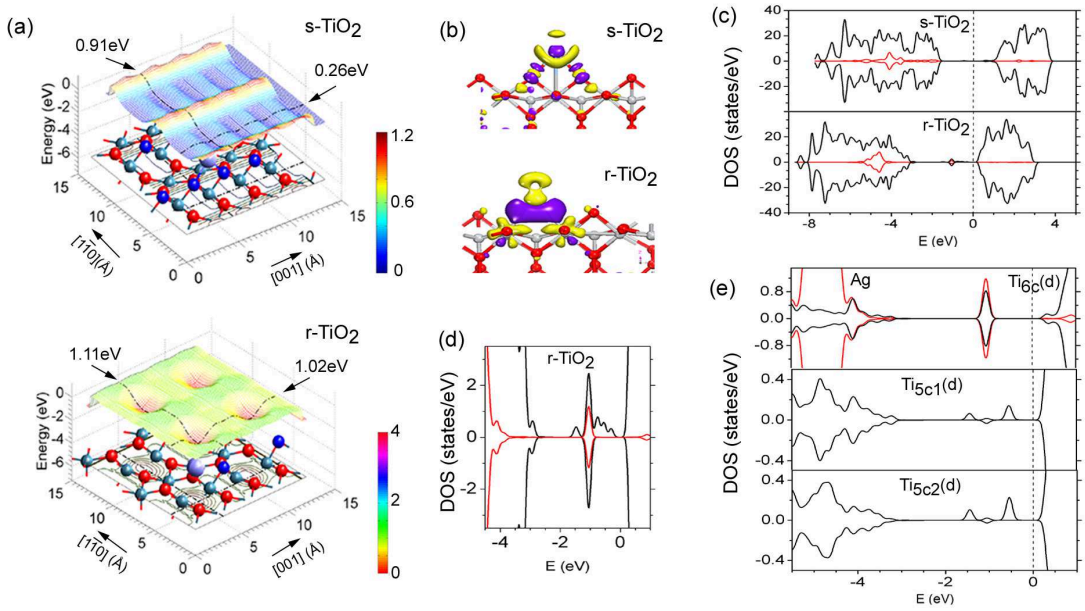

FIG. 5: (a)PES for Ag diffusing on s-/r- TiO_2 surfaces. Activation barriers are labeled for Ag hopping between the minimums along [001] and [110] directions (dashed lines). The spheres in red, blue, and violet color represent O_{2c}, O_{3c}, Ti atoms respectively. (b)Isosurface of the differential charge density, yellow (purple) color denotes diminishing (accumulation) of electrons. (c)LDOS of atoms at the topmost O-Ti_2O_2-O layer calculated from configuration of the most stable adsorption. (d) Enlarged view of (c). (e) LDOS of the adjacent fivefold coordinated Ti atoms around the O_v after Ag adsorption on the r-TiO_2 surface.

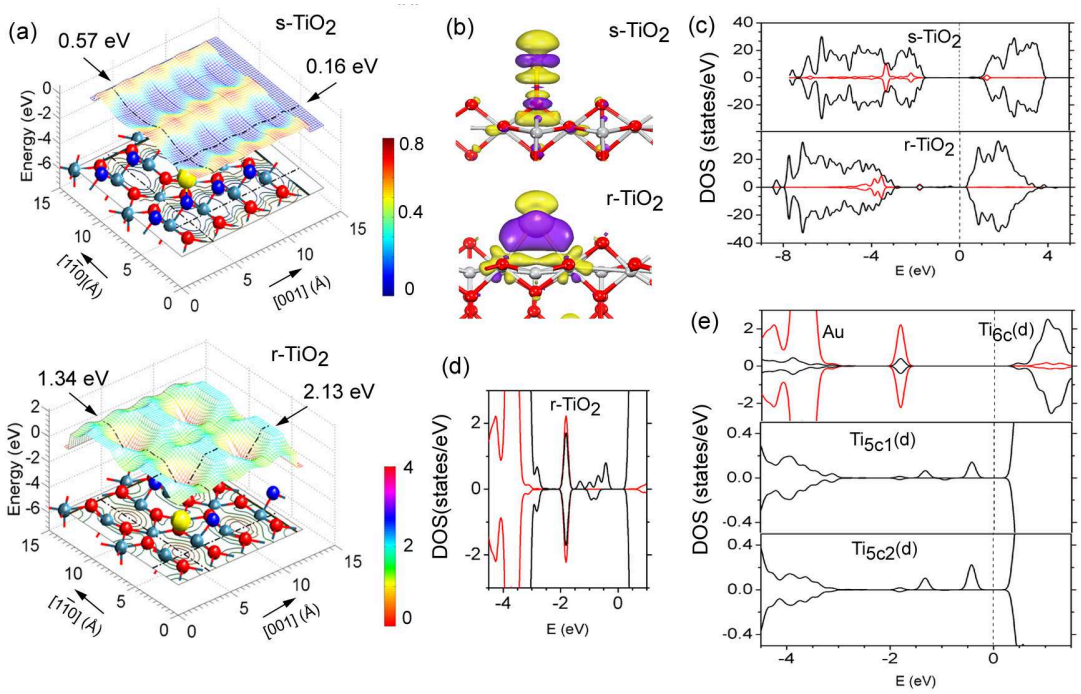

FIG. 6: (a)PES for Au diffusing on *s*-/*r*- TiO_2 surfaces. Activation barriers are labeled for Au hopping between the minimums along [001] and [110] directions (dashed lines). The spheres in red, blue, and violet color represent O_{2c}, O_{3c}, Ti atoms respectively. (b)Isosurface of the differential charge density, yellow (purple) color denotes diminishing (accumulation) of electrons. (c)LDOS of atoms at the topmost O-Ti_2O_2-O layer calculated from configuration of the most stable adsorption. (d) Enlarged view of (c). (e) LDOS of the adjacent fivefold coordinated Ti atoms around the O_v after Au adsorption on the *r*-TiO_2 surface.

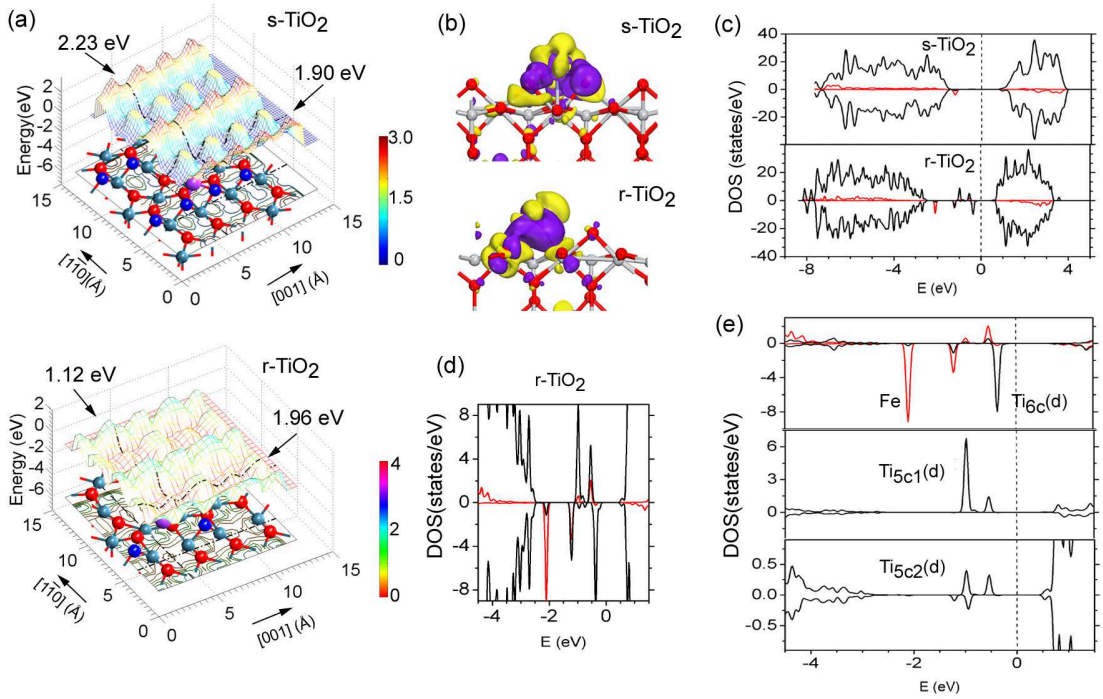

FIG. 7: (a)PES for Fe diffusing on s-/r- TiO_2 surfaces. Activation barriers are labeled for Fe hopping between the minimums along [001] and [110] directions (dashed lines). The spheres in red, blue, and violet color represent O_{2c}, O_{3c}, Ti atoms respectively. (b)Isosurface of the differential charge density, yellow (purple) color denotes diminishing (accumulation) of electrons. (c)LDOS of atoms at the topmost O-Ti_2O_2-O layer calculated from configuration of the most stable adsorption. (d) Enlarged view of (c). (e) LDOS of the adjacent fivefold coordinated Ti atoms around the O_v after Fe adsorption on the r-TiO_2 surface.

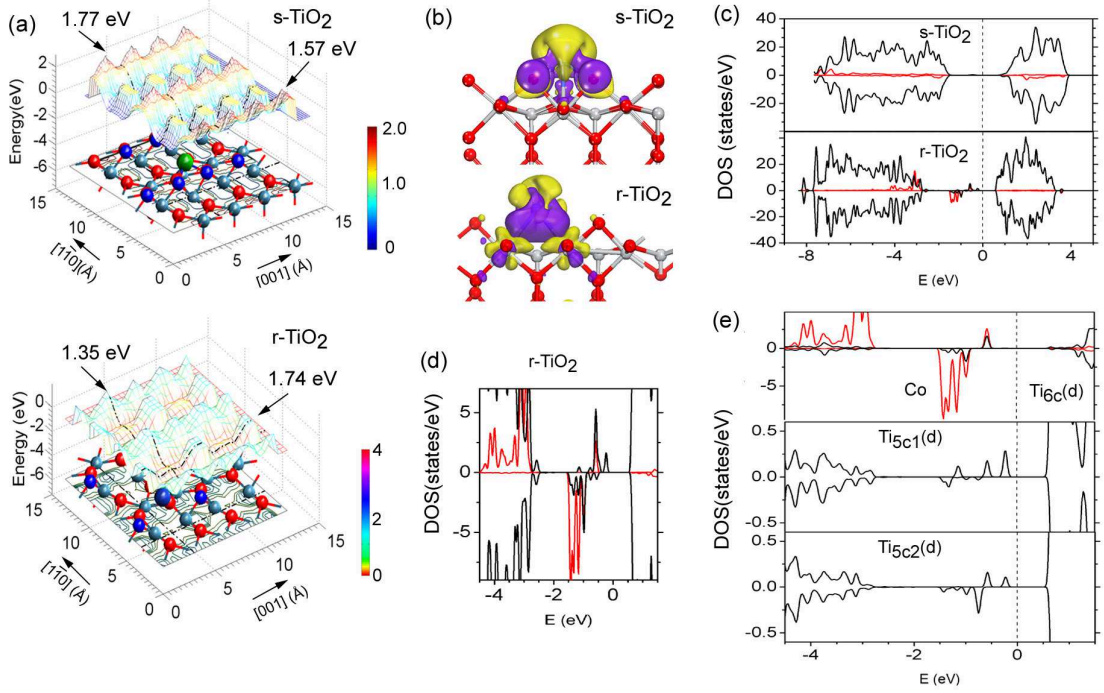

FIG. 8: (a)PES for Co diffusing on *s*-/*r*- TiO_2 surfaces. Activation barriers are labeled for Co hopping between the minimums along [001] and [110] directions (dashed lines). The spheres in red, blue, and violet color represent O_{2c}, O_{3c}, Ti atoms respectively. (b)Isosurface of the differential charge density, yellow (purple) color denotes diminishing (accumulation) of electrons. (c)LDOS of atoms at the topmost O-Ti_2O_2-O layer calculated from configuration of the most stable adsorption. (d) Enlarged view of (c). (e) LDOS of the adjacent fivefold coordinated Ti atoms around the O_v after Co adsorption on the *r*-TiO_2 surface.

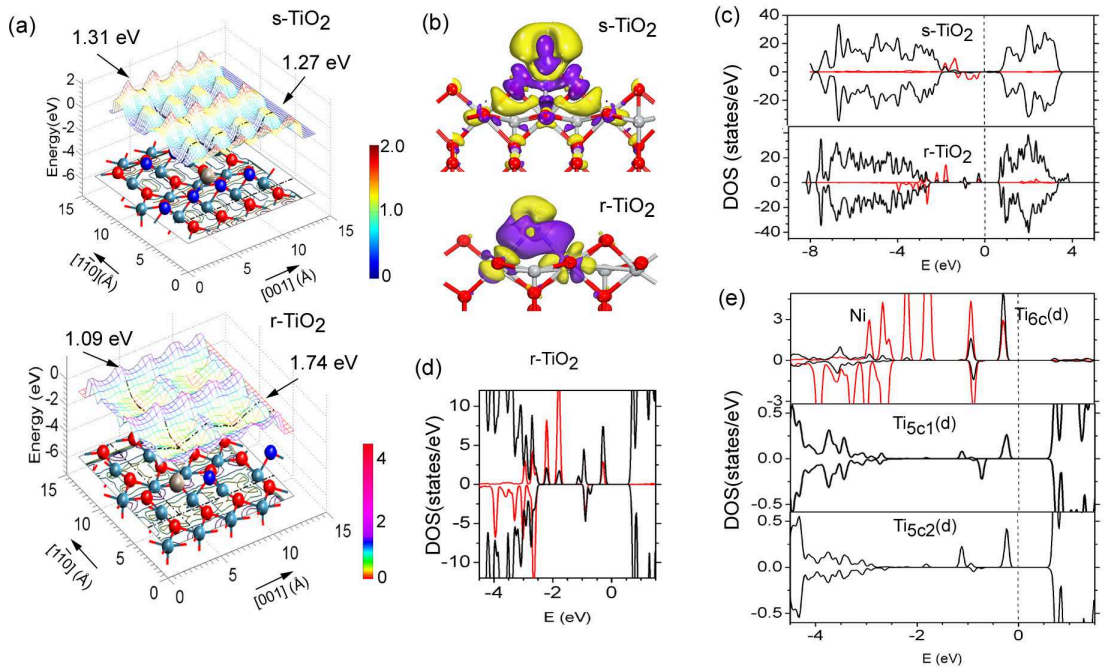

FIG. 9: (a)PES for Ni diffusing on *s*-/*r*- TiO_2 surfaces. Activation barriers are labeled for Ni hopping between the minimums along [001] and [110] directions (dashed lines). The spheres in red, blue, and violet color represent O_{2c}, O_{3c}, Ti atoms respectively. (b)Isosurface of the differential charge density, yellow (purple) color denotes diminishing (accumulation) of electrons. (c)LDOS of atoms at the topmost O-Ti_2O_2-O layer calculated from configuration of the most stable adsorption. (d) Enlarged view of (c). (e) LDOS of the adjacent fivefold coordinated Ti atoms around the O_v after Ni adsorption on the *r*-TiO_2 surface.

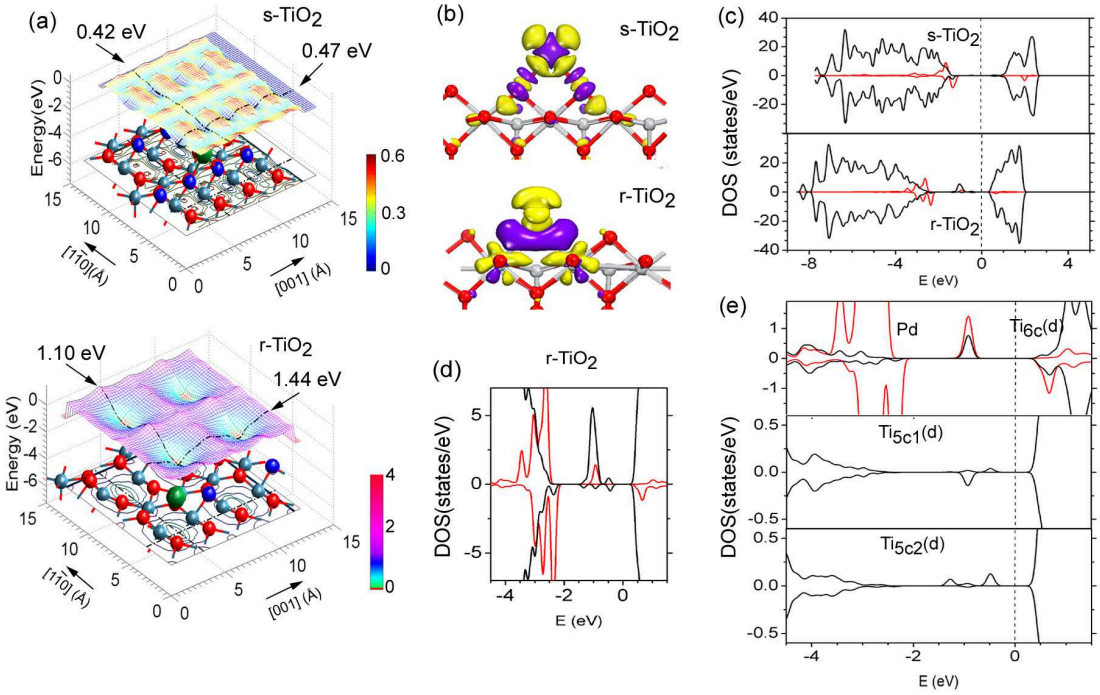

FIG. 10: (a)PES for Pd diffusing on s-/r- TiO_2 surfaces. Activation barriers are labeled for Pd hopping between the minimums along [001] and [110] directions (dashed lines). The spheres in red, blue, and violet color represent O_{2c}, O_{3c}, Ti atoms respectively. (b)Isosurface of the differential charge density, yellow (purple) color denotes diminishing (accumulation) of electrons. (c)LDOS of atoms at the topmost O-Ti_2O_2-O layer calculated from configuration of the most stable adsorption. (d) Enlarged view of (c). (e) LDOS of the adjacent fivefold coordinated Ti atoms around the O_v after Pd adsorption on the r-TiO_2 surface.

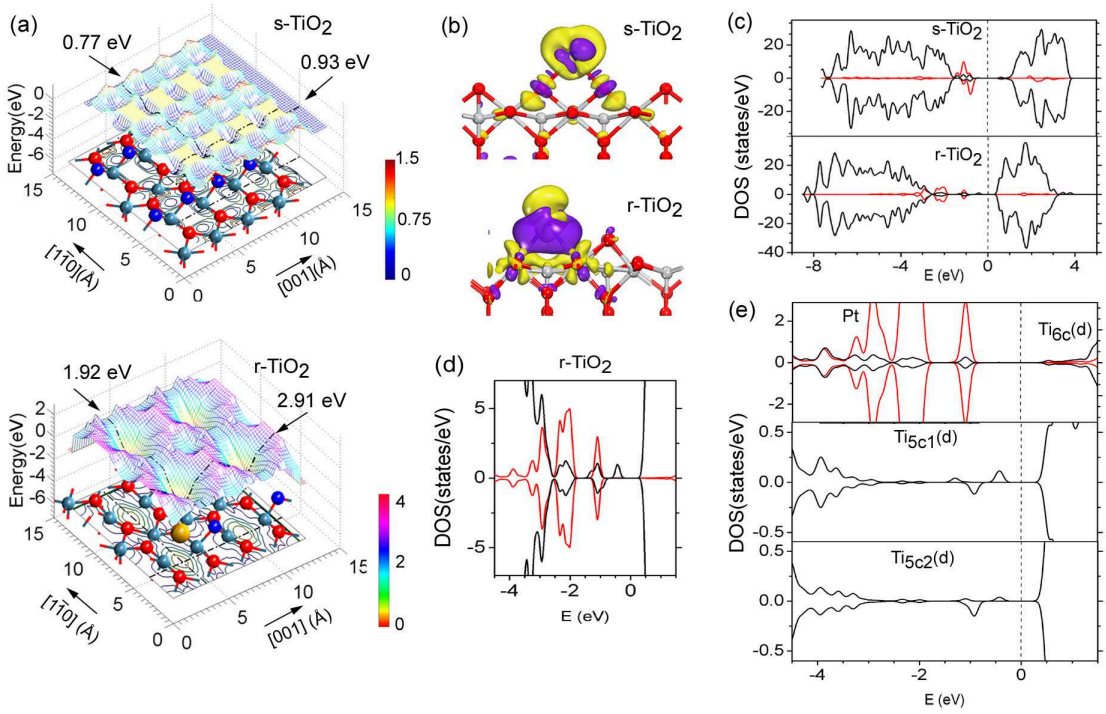

FIG. 11: (a)PES for Pt diffusing on *s*-/*r*- TiO_2 surfaces. Activation barriers are labeled for Pt hopping between the minimums along [001] and [110] directions (dashed lines). The spheres in red, blue, and violet color represent O_{2c}, O_{3c}, Ti atoms respectively. (b)Isosurface of the differential charge density, yellow (purple) color denotes diminishing (accumulation) of electrons. (c)LDOS of atoms at the topmost O-Ti_2O_2-O layer calculated from configuration of the most stable adsorption. (d) Enlarged view of (c). (e) LDOS of the adjacent fivefold coordinated Ti atoms around the O_v after Pt adsorption on the *r*-TiO_2 surface.

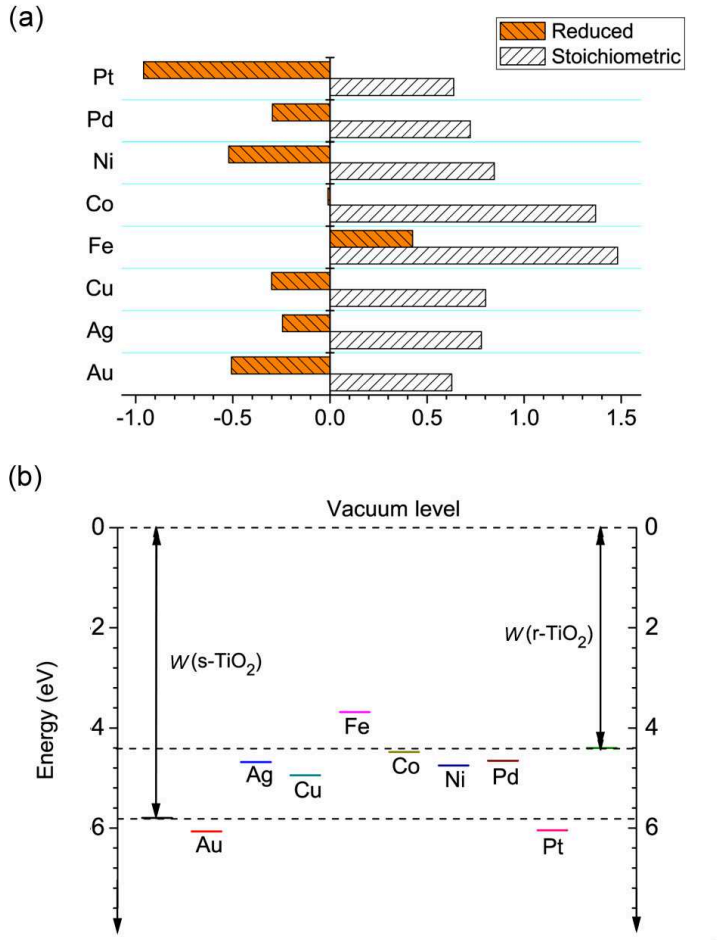

FIG. 12: (a)Comparison of the charged states of TM monomers on stoichiometric and reduced TiO_2 (110) surfaces; (b)Energetic diagram showing the alignment of the electronegativity of TM adatoms with the work function (W) of the stoichiometric and reduced TiO_2 (110) surface, which are calculated with the method provided in Ref. 141

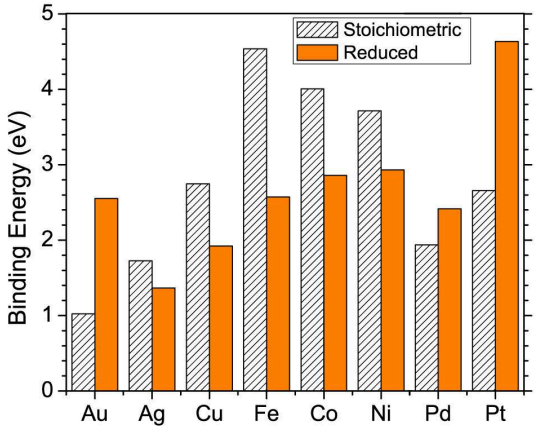

FIG. 13: Binding energy for the adsorption of TM monomers on stoichiometric and reduced TiO_2 (110) surfaces.

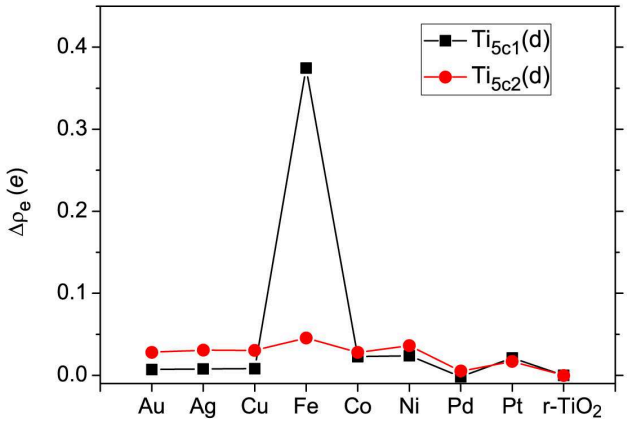

FIG. 14: Increase of the excess electrons distributed on the fivefold coordinated Ti atoms around O_v due to TM adsorption.